

**Exogenous induction of synucleinopathy in transgenic mice –  
An experimental study on the prion-like properties of  $\alpha$ -synuclein**

Dissertation

zur Erlangung des Grades eines  
Doktors der Naturwissenschaften

der Mathematisch-Naturwissenschaftlichen Fakultät  
und  
der Medizinischen Fakultät  
der Eberhard-Karls-Universität Tübingen

vorgelegt  
von

Manuel Schweighauser  
aus Basel, Schweiz

November 2016

---

Tag der mündlichen Prüfung: 23.06.2017

Dekan der Math.-Nat. Fakultät: Prof. Dr. W. Rosenstiel  
Dekan der Medizinischen Fakultät: Prof. Dr. I. B. Autenrieth

1. Berichterstatter: Prof. Dr. M. Jucker  
2. Berichterstatter: Prof. Dr. P. J. Kahle

Prüfungskommission:  
Prof. Dr. M. Jucker  
Prof. Dr. P. J. Kahle  
Prof. Dr. T. Gasser  
Prof. Dr. P. Heutink

---

## Erklärung

Ich erkläre, dass ich die zur Promotion eingereichte Arbeit mit dem Titel:

**„Exogenous induction of synucleinopathy in transgenic mice –  
An experimental study on the prion-like properties of  $\alpha$ -synuclein“**

selbständig verfasst, nur die angegebenen Quellen und Hilfsmittel benutzt und wörtlich oder inhaltlich übernommene Stellen als solche gekennzeichnet habe. Ich versichere an Eides statt, dass diese Angaben wahr sind und dass ich nichts verschwiegen habe. Mir ist bekannt, dass die falsche Angabe einer Versicherung des Eides statt mit Freiheitsstrafe bis zu drei Jahren oder mit Geldstrafe bestraft wird.

Tübingen, den

A handwritten signature in blue ink, appearing to read 'A. Schwab', written over a horizontal dotted line.

Unterschrift



*Für meine Eltern*

---

„If you can meet with triumph and disaster and treat those two imposters just the same“

–Rudyard Kipling

---

## Summary

The accumulation of misfolded proteins into insoluble aggregates is a common feature in a variety of neurodegenerative diseases, and it is thought that the aggregation process plays a central role in the pathogenesis. Parkinson's disease (PD) is the most common movement disorder and characterized by a progressive and selective degeneration of dopaminergic neurons of the substantia nigra. Histopathologically, the hallmark feature of PD is the intracellular deposition of aggregated  $\alpha$ -synuclein ( $\alpha$ S) protein in Lewy bodies. In PD patients, Lewy pathology occurs in a stereotypic pattern, originating in lower brain regions before spreading to higher areas of the brain. Despite a significant amount of research, the mechanism underlying the formation of  $\alpha$ S lesions is still poorly understood. However, recent findings highlight that a nucleation-dependent aggregation mechanism, initially described for prion diseases may also contribute to the propagation of protein aggregation in other neurodegenerative disorders. According to this concept, corrupted protein particles can act as nuclei (or 'seeds') of aggregation and further convert endogenous proteins into their pathological isoforms.

The main objective of this thesis was to study the 'prion-like' properties of  $\alpha$ S to gain further insight into the pathogenesis of PD. In our studies we used different transgenic mouse models of synucleinopathy, which are based on mutations identified in human disease and replicate some aspects of the PD pathology, to probe this theoretical explanation of disease. These mouse lines harbor either the A53T (Tg-9813[A53T] $\alpha$ S and Tg-M83[A53T] $\alpha$ S) or A30P human  $\alpha$ S transgene (Tg-[A30P] $\alpha$ S). Tg-9813[A53T] $\alpha$ S mice develop a severe and early-onset synucleinopathy. On the other hand, both Tg-M83[A53T] $\alpha$ S and Tg-[A30P] $\alpha$ S mice (both being homozygous for the transgene) have a delayed-onset of motor symptoms, whereas the latter tend to exhibit a milder disease phenotype. As shown previously by other research groups, synucleinopathy can be induced by exogenous  $\alpha$ S seeds *in vivo*. Accordingly, we performed a series of inoculation experiments to investigate the seeding effect of pathological  $\alpha$ S.

In a first set of experiments, we assessed whether  $\alpha$ S seeds were still capable of inducing fatal synucleinopathy when treated with formaldehyde. In a previous study, our lab had shown that A $\beta$  seeds resist the inactivation by formaldehyde fixation similar to prions. Therefore, we intracerebrally inoculated young pre-symptomatic mice with extracts from formaldehyde-fixed and fresh-frozen brainstem tissue. Remarkably, in Tg-9813[A53T] $\alpha$ S mice we found that fixed  $\alpha$ S seeds were able to induce synucleinopathy lesions after 30

---

days of incubation. Stimulated by these results, we repeated the experiment in Tg-[A30P] $\alpha$ S mice and incubated until motor symptoms presented. Intriguingly, we found that the pathogenicity of  $\alpha$ S seeds was retained even after formaldehyde fixation prior to the injection. Remarkably, the extract from formaldehyde-fixed brainstem tissue was almost as potent as the fresh-frozen tissue-derived extract with regard to both survival time and pathological  $\alpha$ S load.

The second part of this thesis was focused on investigating whether CSF from mice with synucleinopathy is seeding active. While our group and others had already shown that extracts from mouse brain tissue containing aggregated  $\alpha$ S are potent inducers of synucleinopathy, it is still unclear if extracellular  $\alpha$ S from a bodily fluid is also pathogenic. Our first results revealed an elevated level of  $\alpha$ S in the CSF of symptomatic Tg-[A30P] $\alpha$ S mice. Therefore, we intracerebrally inoculated young presymptomatic Tg-[A30P] $\alpha$ S mice with CSF of spontaneously ill donors. To compare the putative seeding potential of CSF-derived  $\alpha$ S, we additionally performed intracerebral inoculations of the PBS-soluble and PBS-insoluble fractions of brainstem-derived extracts. Our results showed that CSF was not able to induce a synucleinopathy. Likewise, the PBS-soluble fraction failed to induce  $\alpha$ S lesions in Tg-[A30P] $\alpha$ S mice, suggesting a lack of pathogenicity. Conversely, we found a severe induction of synucleinopathy lesions and a significantly reduced life span after inoculation with PBS-insoluble  $\alpha$ S seeds in comparison to the non-tg control inoculum. Although less than 4% of the  $\alpha$ S remained in this fraction, PBS-insoluble  $\alpha$ S seeds were highly seeding-active when compared to the original extract that was diluted to match with the  $\alpha$ S level of both the soluble and insoluble fractions. In addition, we found that the seeded induction of  $\alpha$ S lesions occurred in a concentration-dependent manner.

Finally, in a last set of experiments we have investigated the cross-seeding effect of two mutant  $\alpha$ S pathogens, since *in vitro* studies have indicated that there are indications for structural and functional differences among fibrils of either the mutant A53T or A30P human  $\alpha$ S. When injected into the hippocampus of young presymptomatic Tg-M83[A53T] $\alpha$ S and Tg-[A30P] $\alpha$ S mice, we found that both extracts induced an accelerated disease phenotype with reduced survival times. Moreover, we observed seeded synucleinopathy lesions in each of the recipient mouse strains. However, we found that both the incubation time and the pathology were not different between the tg extract-injected mice in either of the lines indicative of a strong host effect. Therefore, to determine whether the two  $\alpha$ S extracts have a differential cross-seeding capacity, we injected hemizygous Tg-

---

M83[A53T] $\alpha$ S and Tg-[A30P] $\alpha$ S mice that – uninoculated – remain healthy until late adulthood. Intriguingly, both extracts were capable of inducing a *de novo* synucleinopathy in both mouse strains. While we did not find a significant difference in the incubation periods between the two  $\alpha$ S extracts in the hemizygous Tg-M83[A53T] $\alpha$ S mice, the A30P-derived extract was markedly more potent in reducing the survival time than A53T in hemizygous Tg-[A30P] $\alpha$ S mice.

In summary, we were able to study the exogenous seeding mechanism of  $\alpha$ S in different mouse models of synucleinopathy. Our data provide new insight into the persistent nature of  $\alpha$ S seeds that is reminiscent of prions. Moreover, the results of this thesis indicate that PD-linked  $\alpha$ S mutants may dictate functional characteristics *in vivo*. Thus, our findings support the concept that synucleinopathies share several common features with prion diseases. Consequently, Insight into the seeding aspect of the disease could lead to a better understanding of the misfold initiation and spread of the pathogenic protein, ultimately paving the way to therapeutical strategies targeting this particular attribute of PD.



---

## Acknowledgement

I am profoundly grateful for all the support that I had experienced throughout my PhD studies and my time in Tübingen. The following document summarizes four years worth of effort, labor, and struggle, but also great joy and priceless experience. At this point, I would like to thank all of the people that had supported me in one way or another and shared in the success of the scientific work presented in this thesis.

First and foremost, I would like to thank my advisor Professor Mathias Jucker for not only giving me the opportunity to work in his laboratory but also for his aid, guidance, and support throughout my entire work. It has been an absolute privilege for me being part of his group that is well reputed and contributes to the scientific field. I would also like to thank my two other members of the Scientific Advisory Board Professor Manuela Neumann and Professor Philipp J. Kahle for their valuable input and comments on the projects at each stage of the process. Their contribution to the constructive and forward-looking discussions was an integral part of a successful endeavor.

I owe many thanks and appreciation to Dr. Yvonne S. Eisele who initiated the project and taught me the stereotactic injection and to Mehtap Bacioglu who introduced me to the project and helped me with advice and support throughout the entire time. I am also particularly grateful to Bettina Wegenast-Braun and Jasmin Mahler for the project collaboration and fruitful discussions; Stephan Käser, Marius Lambert, and Lisa Häsler for introducing me to the surgical procedure to collect CSF and for the ELISA measurements; Jörg Odenthal, Carina Leibssle, Christian Krüger, and Isolde Breuer for managing mouse work and undertaking the genotyping. I also thank all the other lab members and colleagues of the department Frank Baumann, Natalie Beschorner, Andrea Bosch, Anika Bühler, Karoline Degenhardt, Simone Eberle, Timo Eninger, Sarah Fritschi, Petra Füger, Bernadette Graus, Jasmin Hefendehl, Michael Hruscha, Sonia Mazzitelli, Amudha Nagarathinam, Jonas Nehler, Ulrike Obermüller, Jay Rasmussen, Claudia Resch, Juliane Schelle, Angelos Skodras, Matthias Staufenbiel, Nicholas Varvel, Ulla Welzel, Ann-Christin Wendeln, Renata Werner, Katleen Wild, Jan Winchenbach and Lan Ye for further experimental help and technical support.

The last set of acknowledgments is dedicated to my family and friends. My sincerest thanks and appreciation goes to my parents who have supported me throughout my academic career path. I would also like to thank all my friends who have been a constant source of encouragement.

---

## Table of Contents

Summary	i
Acknowledgment	iv
Table of Contents	v
Acronyms	vii
Chapter	Page
<b>1 Introduction</b>	<b>1</b>
<b>1.1 Aging and disease</b>	<b>1</b>
<b>1.1 Parkinson's disease</b>	<b>2</b>
1.1.1 Neuropathology of PD	3
1.1.2 The role of $\alpha$ -synuclein in PD	4
1.1.2.1 The amyloid state of $\alpha$ S	5
1.1.3 Mouse models of human synucleinopathy	7
1.1.3.1 Tg-[A30P] $\alpha$ S	7
1.1.3.2 Tg-9813[A53T] $\alpha$ S	8
1.1.3.3 Tg-M83[A53T] $\alpha$ S	8
<b>1.2 Prion-like seeding of <math>\alpha</math>-synuclein aggregation</b>	<b>9</b>
1.2.1 The prion principle	9
1.2.2 Experimental seeding of synucleinopathy	10
<b>2 Material and Methods</b>	<b>12</b>
<b>2.1 Animals</b>	<b>12</b>
<b>2.2 CSF collection</b>	<b>13</b>
<b>2.3 Injection material</b>	<b>13</b>
2.3.1 Brain tissue extracts	13
2.3.2 Ultracentrifugation of the brain extracts	13
<b>2.4 Inoculations with brain extracts and CSF</b>	<b>14</b>
<b>2.5 Tissue processing</b>	<b>14</b>
<b>2.6 Histology</b>	<b>15</b>
2.6.1 Neuropathological assessment	15
2.6.2 Imaging and image processing	16
<b>2.7 Biochemistry</b>	<b>16</b>
2.7.1 Quantification of $\alpha$ S by immunoassay	16
2.7.2 SDS-PAGE and immunoblot analysis	17
<b>2.8 Statistics</b>	<b>17</b>

---

<b>3 Results</b>	<b>18</b>
<b>3.1 Seeding activity of formaldehyde-fixed <math>\alpha</math>-synuclein pathogens</b>	<b>18</b>
3.1.1 <i>De novo</i> induction of synucleinopathy with fixed $\alpha$ S seeds	18
3.1.2 Pathogenicity of fixed $\alpha$ S seeds is preserved	19
3.1.2.1 Reduced survival after seeding by fixed $\alpha$ S seeds	19
3.1.2.2 Seed-induced formation of abundant synucleinopathy lesions	21
<b>3.2 Seeding efficacy of CSF in comparison to soluble and insoluble <math>\alpha</math>-synuclein</b>	<b>23</b>
3.2.1 Quantification of brain and CSF $\alpha$ S	23
3.2.1.1 Histopathology and brain $\alpha$ S levels	23
3.2.1.2 Elevated levels of $\alpha$ S in the CSF of diseased mice	25
3.2.1.3 Level of $\alpha$ S in different fractions after ultracentrifugation	25
3.2.2 Lack of pathogenicity of synucleinopathy CSF or soluble $\alpha$ S <i>in vivo</i>	26
3.2.2.1 No differences in incubation times after seeding CSF or soluble $\alpha$ S	27
3.2.2.2 No induction of $\alpha$ S aggregation by CSF or soluble $\alpha$ S	28
3.2.3 Pathological seeding properties of insoluble $\alpha$ S aggregates <i>in vivo</i>	29
3.2.3.1 Reduced incubation time after seeding by insoluble $\alpha$ S seeds	30
3.2.3.2 Formation of abundant synucleinopathy lesions by insoluble $\alpha$ S seeds	31
<b>3.3 Cross-seeding capacities of non-homologous mutant <math>\alpha</math>-synuclein seeds</b>	<b>33</b>
3.3.1 Exogenous cross-seeding is influenced by host	33
3.3.1.1 Both hosts can be seeded by each type of mutant $\alpha$ S seed	34
3.3.1.2 Pattern of neuropathology is predetermined by the host	35
3.3.2 Differential cross-seeding efficiency is revealed in inducible hosts	36
3.3.2.1 Inducible mouse models of synucleinopathy	36
3.3.2.2 Differential seeding capacities of mutant-type $\alpha$ S seeds	37
3.3.2.3 Seeded formation of <i>de novo</i> $\alpha$ S lesions	38
<b>4 Discussion</b>	<b>40</b>
<b>4.1 Formaldehyde resistant <math>\alpha</math>-synuclein seeds</b>	<b>40</b>
<b>4.2 Lack of seeding activity in synucleinopathy CSF</b>	<b>42</b>
<b>4.3 Cross-seeding by Parkinson's disease linked <math>\alpha</math>-synuclein mutants</b>	<b>46</b>
<b>Conclusion</b>	<b>49</b>
<b>References</b>	<b>50</b>
<b>Curriculum Vitae and Bibliography</b>	<b>60</b>

---

## Acronyms

$\alpha$ S	$\alpha$ -synuclein
A30P	Alanine-to-proline substitution at codon 30 of the gene encoding for $\alpha$ -synuclein
A53T	Alanine-to-threonine substitution at codon 53 of the gene encoding for $\alpha$ -synuclein
A $\beta$	$\beta$ -amyloid
AD	Alzheimer's disease
APP	amyloid precursor protein
ANOVA	analysis of variance
CNS	central nervous system
CSF	cerebrospinal fluid
DG	dentate gyrus
DLB	Dementia with Lewy bodies
dpi	days post-inoculation
FPD	familial Parkinson's disease
IHC	immunohistochemistry
LB	Lewy body
LN	Lewy neurite
min	minutes
MSA	Multiple System Atrophy
non-tg	non-transgenic
PBS	phosphate-buffered saline
PD	Parkinson's disease
PDD	Parkinson's disease dementia
PrP	prion protein
pS129	Serine 129 phosphorylation
RT	room temperature
SEM	standard error of the mean
SNCA	gene encoding for $\alpha$ -synuclein

---

TBS	Tris-buffered saline
tg	transgenic
TSE	Transmissible spongiform encephalopathy
v/v	volume per volume percent
wt	wild-type
w/v	weight per volume percent

# 1 Introduction

## 1.1 Aging and disease

The time-dependent decline in cellular fitness and the increase in mortality is what we commonly refer to as aging (López-Otín et al., 2013). Unlike any other organ of the human body, the brain possesses a very high vulnerability response to oxidative, metabolic, and ionic stress that cells experience during a lifetime. In individuals, the process of healthy aging does not necessarily occur synchronously in all cell types resulting in a disparity between physical and mental health. Since most of the neurons are post-mitotic cells (in contrast to other cell types), adapting to these changes is key to a healthy aging process. Despite relentless research dedicated to unraveling the molecular basis of aging, there has been no popularly accepted mechanism to describe senescence (Lenart and Krejci, 2016).

When neurons fail to adjust to age-dependent changes, the balance is likely to shift to a pathological state, where damaged proteins and DNA accumulate inside and outside the cells, impairing cellular function and ultimately degenerate. Dementia represents a significant part of the neural aging disorders. The irreversible degeneration of cells in the nervous system is the main disease characteristic, which clinically manifests in a progressive cognitive decline among affected individuals. The prevalence of developing dementia increases dramatically with age. Whether or not a person subjects to a neurodegenerative disease is, however, not solely determined by the individual's age, but is counteracted or contributed by environmental factors, their family history and genetic background. Nonetheless, the overall prevalence of contracting a form of dementia is about 10% during a lifespan (Loy et al., 2014).

The global average life expectancy has more than doubled since the beginning of the 20th century, which has led to an overall aging of the population (Oeppen and Vaupel, 2002). As a result, the prevalence of neurodegenerative diseases has increased significantly, afflicting individuals across all segments of society and posing a challenge for health institutions worldwide. Therefore, the intended aims of current neuroscience research should be focused on understanding the molecular and cellular mechanisms underlying (brain) aging in health and disease.

## 1.2 Parkinson's disease

In 1817, James Parkinson published a clinical essay describing a wasting disorder affecting the locomotor system of humans (“shaking palsy”) (Parkinson, 2002, Lees, 2007). Even though many before him had forestalled the topic, his clear clinical description helped to draw the attention of physicians worldwide to the illness that later would carry his name. Now, almost two hundred centuries later, Parkinson's disease (PD) is known to be the second most common degenerative disease of the nervous system and the most common movement disorder affecting people all over the globe (Lesage and Brice, 2009). The clinical syndrome is characterized by a panoply of motor signs such as bradykinesia (i.e. slowness of voluntary movement), rigidity, resting tremor, and instability of gait, as well as non-motor symptoms like hyposmia, sleep disturbances, and depression that may affect the patient's quality of life tremendously. Often, the non-motor phenotype precedes the motoric facet of the disease (Lang and Lozano, 1998a, 1998b). The average age of onset is between 50 and 70 years (de Rijk et al., 1995, de Laud and Breteler, 2006). The disease progresses slowly and terminates with death 10 to 20 years later. The prevalence of PD increases with advancing age from 1% to 2% to up to 4% to 5% in people above the age of 85 (de Rijk et al., 1995). The lifetime incidence of developing PD is 2% (Pringsheim et al., 2014). Worldwide, an estimated 7 million people are suffering from PD ([www.pdf.org](http://www.pdf.org)). The non-heritable idiopathic cases contrast the rare familial forms of PD (FPD), which are caused by single gene mutations and constituting less than 10% of all cases (Thomas et al., 2007). Molecular genetic analysis of these families has revealed mutations in more than 10 genes (Corti et al., 2011, Houlden and Singleton, 2012, Ferreira and Massano, 2016), whereas, the etiology of sporadic PD is far more complex with many factors contributing to the age of onset, disease progression and duration.

### 1.2.1 Neuropathology of Parkinson's disease

The neuropathology of PD is characterized by the progressive and selective loss of dopaminergic neurons in the substantia nigra pars compacta (SNc) of the midbrain (overviewed in Figure 1) associated with intracellular inclusions called Lewy bodies (LBs) and Lewy neurites (LNs) in surviving neurons (Gibb and Lees, 1988, Fearnley and Lees, 1991, Forno et al., 1996). LBs are round eosinophilic, proteinaceous deposits consisting primarily of filamentous  $\alpha$ -synuclein ( $\alpha$ S) aggregates, neurofilaments, and ubiquitin, and are considered to be a hallmark feature of neurodegeneration (Forno, 1996, Spillantini et al., 1997).

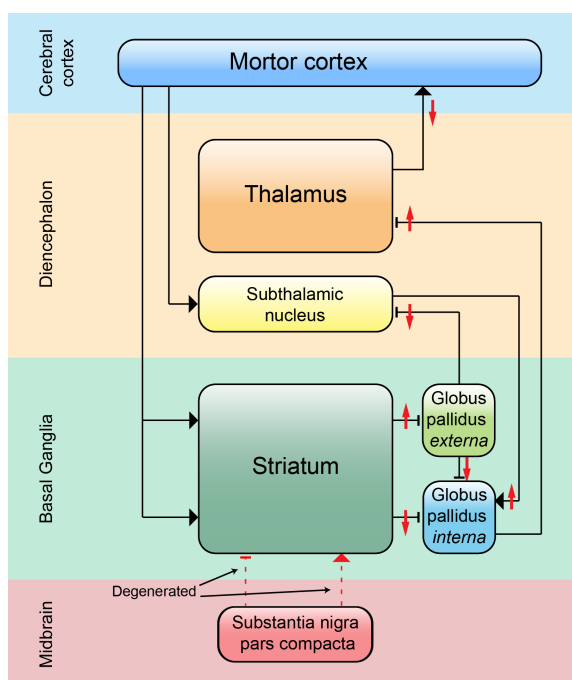


**Figure 1.** Corticostriatal pathway in Parkinson's disease. Degeneration of the dopaminergic neurons (dashed lines) from the substantia nigra pars compacta (SNc) projecting to the striatum leads to a diminished inhibition of globus pallidus *interna* (direct pathway). Hence, thalamic excitation of the motor cortex is less likely. Changes are indicated with red arrows (up: increase; down: decline). (After DeLong, 1990.)

Apart from PD, LBs are the main pathological characteristic in at least two other neurodegenerative diseases, dementia with LB (DLB) and multiple system atrophy (MSA) that are collectively known as "synucleinopathies" (Spillantini et al., 1997, Spillantini et al., 1998, Goedert et al., 2013). In PD patients,  $\alpha$ S deposition and LB pathology seems to occur in a stereotypic manner along interconnected neuronal pathways, making it possible to distinguish six stages of  $\alpha$ S pathology (Braak et al., 2003, Braak et al., 2009). At first, deposition of  $\alpha$ S occurs in the anterior olfactory nucleus and the dorsal motor nuclei of the vagal and glossopharyngeal nerves in the brainstem (stage 1). In stage 2, LBs and LNs are observed in the medulla oblongata and the pontine tegmentum. Then, the  $\alpha$ S lesions spread towards the amygdala and the SNc in the midbrain (stage 3). At this stage, usually the first motor symptoms begin to appear. By stage 4, the pathology has reached the temporal



mesocortex as the first cortical region. Finally, in the last two stages the pathology attain the neocortex including high order sensory association areas and areas of the premotor cortex (stages 5 and 6) (Braak et al., 2003, Braak et al., 2009). Conversely, there is emerging evidence suggesting an initiation of disease in the gastrointestinal tract including the autonomic nervous system and the enteric nervous system (Hawkes et al., 2007, Hawkes et al., 2009).

At present, there is no cure for PD, and classic therapeutic approaches are rather limited to treating the disease symptoms than meeting the root of the illness (overviewed in Hickey and Stacy, 2011). Notwithstanding the benefits of current therapies for thousands of patients, new therapeutic strategies should be aimed at modifying the course of the disease (reviewed in Eisele et al., 2015). Likewise, reliable diagnostic means need to be established to determine PD at an early stage, where therapies are most effective. Therefore, it is of paramount importance to fully unravel and understand the etiology and pathogenesis of PD to open up new ways for novel, cause-directed therapies.

### **1.2.2 The role of $\alpha$ -synuclein in PD**

Almost 100 years after James Parkinson had published his famous forward-looking clinical essay, Friedrich Heinrich Lewy described in 1912 the intracellular inclusions in both the cell bodies (i.e. LBs) and cell processes (i.e. LNs) of neurons (Lewy, 1912). Nonetheless, it was not until the late 1990s when two findings brought the focus of work on the pathogenesis of PD to the protein  $\alpha$ S (see Fig. 2) (Polymeropoulos et al., 1997, Spillantini et al., 1997). The identification of *SNCA* mutations led to the first direct link between genetics and LB pathology observed in hereditary as well as idiopathic PD (Polymeropoulos et al., 1996, Polymeropoulos et al., 1997). The subsequent discovery of  $\alpha$ S in LBs in the brains of sporadic PD patients further supported the role of the protein in the pathobiology of the disease (Spillantini et al., 1997). To date, a total of six point mutations in the  $\alpha$ S gene have been identified to cause rare familial forms of PD (Polymeropoulos et al., 1997, Krüger et al, 1998, Zarranz et al., 2004, Appel-Cresswell et al., 2013, Proukakis et al., 2013, Lesage et al., 2013, Pasanen et al., 2014). By far the most frequent *SNCA* mutation in humans is the alanine-to-threonine substitution at codon 53 in the protein sequence (A53T) (Polymeropoulos et al., 1997). Apart from A53T, the alanine-to-proline substitution at position 30 (A30P) has been known and studied for almost two decades (Krüger et al, 1998). Importantly, duplications and triplications of wild-type (wt) *SNCA* also cause FPD (Chartier-

Harlin et al., 2004, Singleton et al., 2003), whereas the multiplicity of the gene locus correlates positively with the clinical manifestation of the disease suggesting a causal link between *SNCA* gene dosage and disease phenotype (Ibáñez et al, 2004).

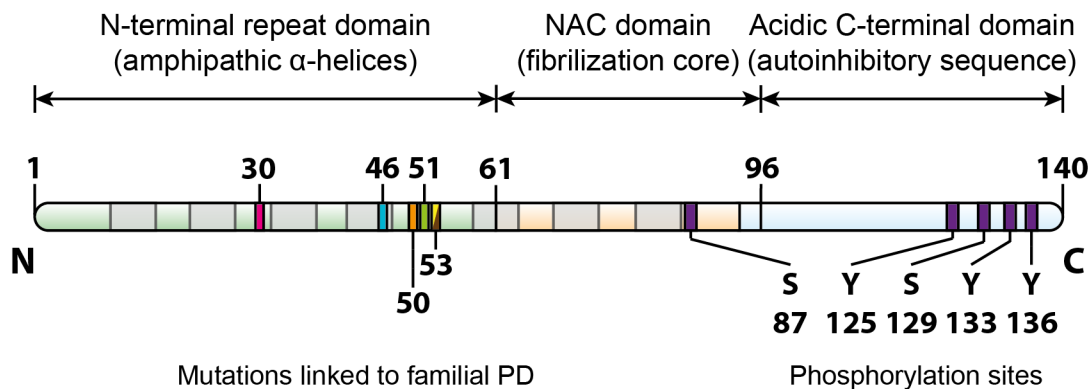


**Figure 2.** *The structure of  $\alpha$ -synuclein.* The protein folds into two  $\alpha$ -helices upon binding to lipid membranes conferred by seven imperfect 11-residue repeats (KTKEGVXXXX) that include the highly conserved KTKEGV consensus sequence (light gray boxes). The N-terminus (light green; amino acids 1 to 60) contains with five repeat sequences. The hydrophobic middle segment, i.e. non-amyloid- $\beta$  component of AD amyloid (NAC), confers the propensity to fold into a  $\beta$ -sheet secondary structure (light orange; 61 to 95). The highly negatively charged C-terminal domain is not implicated in membrane binding and is intrinsically disordered (light blue; 96 to 140). Interestingly, all of the mutations associated with PD – A53T, A30P, E46K, H50Q, G51D, and A53E – lie within the N-terminal region. Conversely, the C-terminus contains the majority of post-translational modifications including phosphorylation at 4 residues (Tyr 125, Ser 129, Tyr 133, and Tyr 136). (Modified from Breydo et al., 2012.)

Besides its role in disease,  $\alpha$ S has been implicated in various cellular processes (over-viewed in Bendor et al, 2013). Nonetheless, the physiological function remains elusive. Therefore, over the last decade research has been focused particularly on elucidating the structure and function of this protein (for a review see Bennett, 2005).

### 1.2.2.1 The amyloid state of $\alpha$ -synuclein

The aggregation of misfolded proteins is a common feature of many neurodegenerative diseases, including  $\alpha$ S in PD, the amyloid- $\beta$  ( $A\beta$ ) peptide in Alzheimer's disease (AD) or the microtubule associated protein tau in frontotemporal dementia and AD (reviewed in Jucker and Walker, 2013). In fact, many such proteinopathies have been described so far (Bayer, 2013). In line with this, there is compelling evidence that  $\alpha$ S aggregation is the critical step in the pathogenesis of PD and other synucleinopathies. The mechanism un-

derlying protein aggregation is a multi-step process involving several off-pathway intermediate forms whose generation is given by their respective kinetics (Fig. 3).

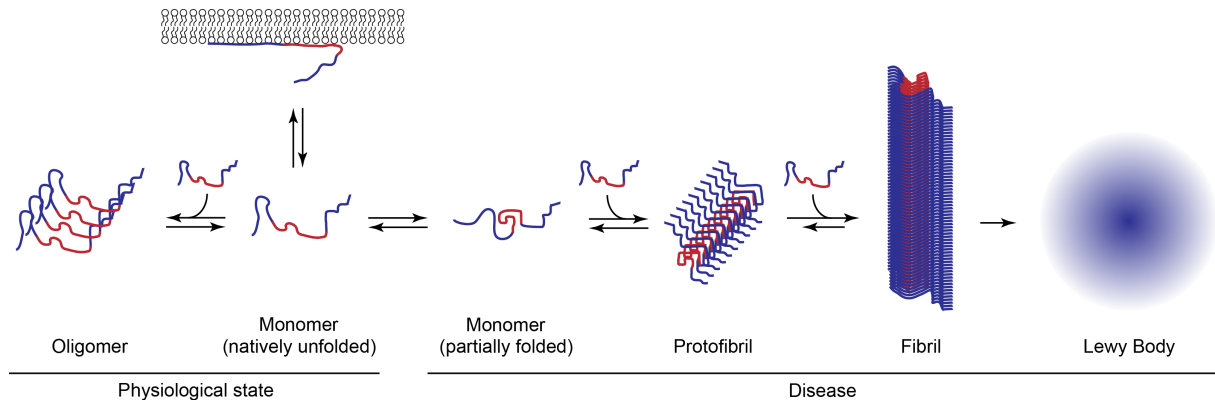


**Figure 3.** Mechanism of  $\alpha$ -synuclein aggregation and fibrillogenesis. In a native state,  $\alpha$ S appears to be present as an unfolded monomer in solution or in an  $\alpha$ -helical conformation when bound to a membrane. Soluble oligomers of unfolded  $\alpha$ S might thereby represent an on-pathway condition. On the other hand, the non-native aggregation of  $\alpha$ S involves a misfolded intermediate that escapes the cellular clearance machinery and is prone to oligomerize into  $\beta$ -sheet rich protofibrils, which may give rise to more stable amyloid fibrils. Finally, the pathological aggregation results in the formation of the bulky, cytoplasmic inclusions seen as LBs. (Modified from Lashuel et al., 2013.)

*In vitro*, natively unfolded  $\alpha$ S monomers have a high intrinsic propensity to form fibrils. Thereby the formation of amyloid  $\beta$ -sheet structures involves a conformational transition (i.e. “misfolding”) of the protein (Uversky et al., 2001). Under physiological condition, there is an equilibrium state between the natively unfolded and the misfolded  $\alpha$ S conformation. However, the misfolding of  $\alpha$ S can be induced or inhibited by several intrinsic or extrinsic factors (reviewed in Uversky, 2007). For example, several different posttranslational modifications have been thought to be important modifiers of protein aggregation (reviewed in Barrett, 2015). These modifications include phosphorylation, ubiquitination, oxidation, and nitration. Of note,  $\alpha$ S phosphorylation appears to be significantly increased throughout synucleinopathy lesions (Fujiwara et al., 2002, Paleologou et al., 2010, Hejjaoui et al., 2012). In fact, about 90% of the insoluble  $\alpha$ S was found to be phosphorylated at Ser 129 (pS129) making it a consistent marker of  $\alpha$ S pathology (Fujiwara et al., 2002, Anderson et al., 2006). Likewise, sequence truncations are typical modifications, and C-terminally truncated  $\alpha$ S has been identified in LBs in addition to the full-length protein (Baba et al., 1998, Li et al., 2005, Liu et al., 2005). Interestingly, both multiplication and PD-associated point mutations have been implicated in altering  $\alpha$ S aggregation (Chartier-Harlin et al., 2004,

Conway et al., 1998). Strikingly, an increased protein expression as caused by a triplication of *SNCA* is enough to cause an imbalance of the regulatory pathways and thereby shifting the equilibrium towards an increase in the accumulation of insoluble  $\alpha$ S (Chartier-Harlin et al., 2004). On the other hand, *SNCA* mutations have been shown to affect the aggregation kinetics of the protein *in vitro* (Conway et al., 1998, Giasson et al., 1999, Narhi et al., 1999, Li et al., 2001). While the two mutations A53T and E46K have been shown to enhance the formation of mature fibrils, the A30P mutant significantly slows down the fibrilization rate (Li et al., 2002, Li et al., 2001). On the other hand, A30P does form oligomers more rapidly than the wt protein (Conway et al., 2000b).

### **1.2.3 Mouse models of human synucleinopathy**

By today, numerous transgenic mouse models have been developed to investigate the physiological and pathological role of  $\alpha$ S *in vivo*. To model PD in mice, the identification of disease-associated mutations in  $\alpha$ S has played a significant role. For instance, two autosomal dominant mutations in  $\alpha$ S, A53T (Polymeropoulos et al., 1997) and A30P (Krüger et al., 1998), were found to cause early-onset FPD. In addition to  $\alpha$ S gene overexpression, models expressing either A53T or A30P mutant human  $\alpha$ S under various promoters are commonly used (summarized in Crabtree and Zhang, 2012). Even though none of these models exhibit dopaminergic cell loss in the substantia nigra, they have been proven a valuable tool to study the pathophysiology of synucleinopathies recapitulating neuronal  $\alpha$ S pathology as seen in humans (Matsuoka et al., 2001, Kahle, 2007). In the following, three transgenic mouse models of synucleinopathy that were used in this thesis are described.

#### **1.2.3.1 Tg-[A30P] $\alpha$ S**

The first transgenic mouse line making use of a PD-linked  $\alpha$ S mutation was the Tg-[A30P] $\alpha$ S (Kahle et al., 2000a, 2000b). This model has the transgene expressing the A30P mutant of human  $\alpha$ S under the control of the brain neuron-specific murine Thy-1 promoter. In homozygotes, the expression level of the transgene has been described to be two-fold higher relative to the endogenous  $\alpha$ S level (Kahle et al., 2000a). Lewy like pathology of hyperphospho- and proteinase K-resistant  $\alpha$ S inclusions are observed predominantly in the brainstem and spinal cord. Despite the widespread transgenic expression of  $\alpha$ S throughout the brain, there is no proteinase K-resistant  $\alpha$ S in the substantia nigra or stria-

tum. Homozygous Tg-[A30P] $\alpha$ S mice further display a progressive locomotor impairment in the second year of life (Neumann et al., 2002). The motor phenotype is characterized by a hunched posture and spastic paralysis of the hind limbs. By contrast, hemizygotes develop the same pathology at least 1 year later than homozygous Tg-[A30P] $\alpha$ S mice (Neumann et al., 2002).

### **1.2.3.2 Tg-9813[A53T] $\alpha$ S**

The Tg-9813[A53T] $\alpha$ S mouse line expresses the human  $\alpha$ S transgene harboring the A53T point mutation under the control of the brain neuron-specific murine Thy-1 promoter (van der Putten et al., 2000). This line was generated on a C57Bl/6 background and expresses the transgene heterozygously. These mice show an early onset of disease between 2-6 months of age with dramatic decline of motor function. Most of the pathological changes are found in the spinal cord with a pronounced degeneration of motor neurons. On the other hand, the nigrostriatal system is not affected, although ubiquitin-positive  $\alpha$ S inclusions are also observed in the telencephalon, brainstem, and cerebellum (van der Putten et al., 2000).

### **1.2.3.3 Tg-M83[A53T] $\alpha$ S**

The third mouse model, Tg-M83[A53T] $\alpha$ S, harbors also the A53T mutation in the human  $\alpha$ S transgene (Giasson et al., 2002). However, in these mice the transgene is under the control of the mouse prion promoter (*Prnp*). The transgenic over-expression is stated to be 2.5- to 30-fold relative to the endogenous  $\alpha$ S level, depending on the brain region. In contrast to the other two lines, this model was generated on a C57Bl/C3H mixed background. In homozygous mice, the motor phenotype occurs at middle age and manifests in a hunched back, freezing behavior and a (fatal) paralysis in all four limbs. Hemizygous animals develop a similar phenotype, however, the onset occurs in late-life (>22 months). A high density of  $\alpha$ S inclusions are found in the spinal cord, brainstem, cerebellum (except granular and Purkinje cells), thalamus, and striatum. In addition, pronounced astrogliosis is observed in affected areas. In homozygous mice the pathology is reported to occur at 7 months of age.

## 1.2 Prion-like seeding of $\alpha$ -synuclein aggregation

### 1.2.1 The prion principle

The best known examples of protein misfolding within the nervous system are the transmissible spongiform encephalopathies (TSE) (Collins et al., 2004, Aguzzi et al., 2008a, Prusiner, 1998). TSEs, or prion diseases, are a group of fatal degenerative disorders affecting the central nervous system (CNS) in many mammals (Collins et al, 2004). Prion diseases include scrapie in sheep and goat, bovine spongiform encephalopathy (BSE) in cattle, and Creutzfeldt-Jakob disease (CJD) in humans. It was in the 1960s when scientists led by D. C. Gajdusek, C. J. Gibbs, and M. Alpers were able to transmit experimentally kuru (a human type of TSE) to apes and disclosed the infectious nature of a human brain disorder (Gajdusek et al, 1966, Alpers, 2007). Fifteen years later, S. B. Prusiner and colleagues proposed the composite term *prion* – from “proteinaceous” and “infectious” – to describe the causative agent for scrapie (Prusiner, 1982a).

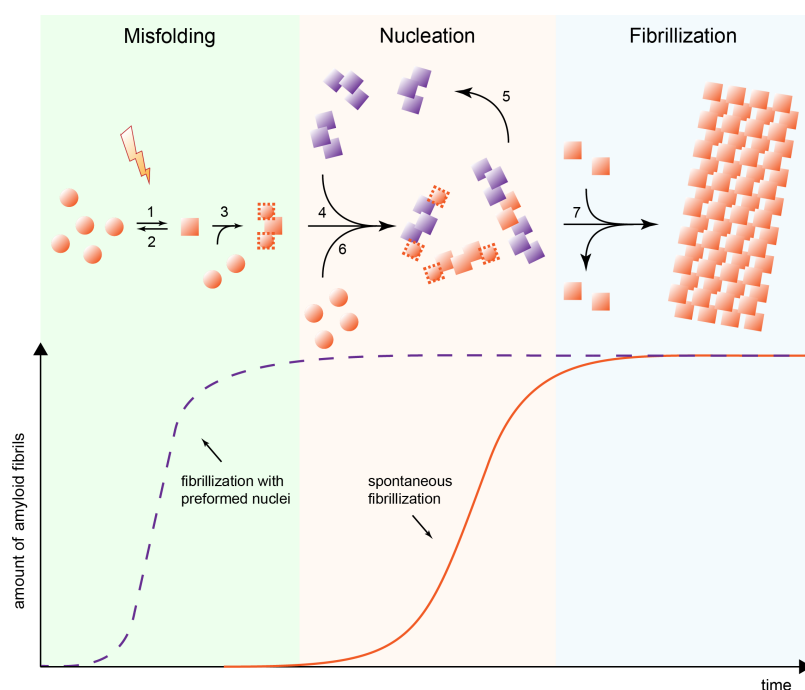


**Figure 4.** Model of nucleation-dependent fibrillization mechanism. The re- or misfolding (step 1) of a native protein (sphere) into its abnormally folded isoform (cube) is a stochastic event (2) since the abnormal form is either unstable or sensitive to clearance and therefore unfavourable. The abnormal form interacts with the native proteins and binds them by conformational conversion (3). Therefore, the formation of a stable nucleus (4) is a time-dependent process (corresponding to the lag time of the orange curve). Once a nucleus (or “seed”) has formed, the protein aggregate can grow by incorporating monomeric protein (6) until a steady state is reached (7). However, the growing fibril may break into smaller fragments that further act as seeds (5) and thusly, accelerate the rate of fibrillization substantially (purple curve). (After Naiki and Geiyo, 1999.)

Despite the clinical and pathological heterogeneity, all prion diseases share a unifying mechanism of pathogenesis following the “protein-only” hypothesis (see Fig. 4). Central to TSE pathogenesis is the conformational transformation (i.e. “misfolding”) of normal, cellular PrP (PrP<sup>C</sup>) into a disease-associated,  $\beta$ -sheet-rich scrapie isoform of PrP, known as PrP<sup>Sc</sup> (Prusiner, 1998, Cohen and Prusiner, 1998). Once generated, PrP<sup>Sc</sup> acts as a template to promote the conversion of PrP<sup>C</sup> into nascent PrP<sup>Sc</sup> (Prusiner, 1998). As a result of this self-perpetuating mechanism, the pathology spreads throughout the brain, neurons degenerate and the disease progression sustains (Prusiner, 2013). Although PrP<sup>C</sup> and PrP<sup>Sc</sup> share the same amino acid sequence, they differ from each other in several facets. Unlike PrP<sup>C</sup>, PrP<sup>Sc</sup> is insoluble, partially resistant to proteinase digestion and presents some unconventional properties, such as resistance to high temperatures, formaldehyde fixation, or UV-irradiation (Cohen and Prusiner, 1998, Aguzzi et al., 2008b). Moreover, PrP<sup>Sc</sup> has been shown to adopt a wide range of structurally different morphologies. These ‘strains’ arise from alternative conformations of the same protein and are the molecular basis of the phenotypic variability observed in TSEs (Morales et al., 2007, Aguzzi et al., 2007, Cobb and Surewicz, 2009). Prion strains can be classified by different parameters. In transmission experiments, prion strains consistently develop a disease with distinct incubation times after inoculation, clinical signs, distribution of brain pathology, and severity of spongiosis in the brain of affected animals (Aguzzi et al., 2007, Collinge and Clarke, 2007). Most importantly, these characteristics are stably and faithfully propagated in serial passages. Although the novel principle underlying protein aggregation and disease propagation was initially discovered in prion diseases (a rather “exotic” subset of degenerative diseases), it soon emerged that other age-related neurodegenerative disorders – including AD and PD – might share the same biological concept for disease pathogenesis (Prusiner, 2012, Walker and Jucker, 2015). In stark contrast to the infectious nature of prions, however, there is no definitive evidence to support the idea for a person-to-person transmission of PD (or other proteinopathies). Therefore, to encompass all other degenerative diseases it has been proposed that the term *prion* should be redefined (Walker and Jucker, 2015).

### 1.2.2 Experimental seeding of synucleinopathy

The first evidence suggesting that  $\alpha$ S pathology can propagate from cell-to-cell in a prion-like manner emerged from two studies on postmortem brain tissue from PD patients who had previously received fetal mesencephalic tissue transplants one to two decades before

their death (Kordower et al., 2008, Li et al., 2008). Surprisingly, some of these nigral tissue grafts showed Lewy body-like pathology similar to that in the host brain. Hence, it is conceivable that aggregated  $\alpha$ S transferred from host-to-graft, where it seeded the aggregation of soluble  $\alpha$ S. Likewise, the previously described staging of neuropathology in PD brains, according to which  $\alpha$ S lesions spread to interconnected brain regions following anatomical pathways, is reminiscent of a prion-like mechanism of disease propagation (reviewed in Visanji et al., 2013). To test the hypothesis of prion-like seeding, researchers have performed transmission experiments, injecting misfolded proteins into the brains of rodents. The first experimental transmission of non-prion diseases was demonstrated in tg mouse models for cerebral  $\beta$ -amyloidosis (Meyer-Luehmann et al., 2006) and tauopathy (Clavaguera et al., 2009). In 2011, Mougenot and colleagues reported the experimental induction of synucleinopathy in  $\alpha$ S tg mice by intracerebral inoculation with brain homogenates derived from old and sick tg animals (Mougenot et al., 2012). In line with the model for seed-dependent fibrillization (see Fig. 4), the exogenous induction led to an accelerated onset of neurological symptoms and a reduced survival compared with that of uninoculated tg controls. Moreover, subsequent work could demonstrate that exogenously induced  $\alpha$ S pathology propagates within the CNS from the site of injection to interconnected regions far beyond (Luk et al., 2012a). Also, it was shown that synthetic fibrils assembled from recombinant human  $\alpha$ S alone are sufficient to induce Lewy-like pathology that ultimately leads to a fatal neurological phenotype in mice, whereas  $\alpha$ S<sup>-/-</sup> mice inoculated with  $\alpha$ S aggregate-containing extract were resistant to the disease (Luk et al., 2012a). Thus, these findings are consistent with the protein-only hypothesis of prion-like disorders. However, despite several similarities between the prion protein and  $\alpha$ S, there is no evidence that synucleinopathy is contagious except in experimental paradigms.

Taken together, evidence is mounting that the prion-like spread of misfolded  $\alpha$ S proteins are the cause of synucleinopathies like PD. However, this mechanism is still not fully understood and remains subject to debate. If it holds true that  $\alpha$ S plays a central role in the pathological process then therapies should be targeted at stopping the aggregation in order to slow down or prevent the disease progression. Therefore, understanding the pathogenesis of the disease at the cellular and molecular levels is critical for discovering, developing, and implementing methods to improve PD treatment.



---

## 2 Material and Methods

### 2.1 Animals

Transgenic mice were used from the following lines: Tg-[A30P] $\alpha$ S (Kahle et al., 2000a, Neumann et al., 2002), Tg-M83[A53T] $\alpha$ S (Giasson et al., 2002), and Tg-9813[A53T] $\alpha$ S (van der Putten et al., 2000). Tg-[A30P] $\alpha$ S mice, which express human  $\alpha$ S with the A30P mutation under the control of the mouse Thy1-promoter, were kindly provided by Prof. P.J. Kahle (University of Tübingen). Homozygous Tg-[A30P] $\alpha$ S mice developed a severe and fatal motor phenotype spontaneously with a late-onset of disease ( $18\pm 2$  months), whereas heterozygous animals did not show any motor signs by the age of 18 months. Tg-M83[A53T] $\alpha$ S mice, which express human  $\alpha$ S with the A53T mutation under the control of the mouse prion protein promoter, were purchased from The Jackson Laboratory. Homozygous Tg-M83[A53T] $\alpha$ S mice developed spontaneously a very rapid disease phenotype terminating in a complete paralysis of both fore and hind limbs by mid-life ( $14\pm 3$  months). On the other hand, heterozygous Tg-M83[A53T] $\alpha$ S mice did not show any signs of neurological dysfunction by the age of 24 months. Tg-9813[A53T] $\alpha$ S mice, which express human  $\alpha$ S with the A53T mutation under the control of the mouse Thy1-promoter, were graciously provided by Dr. D.R. Shimshek (Novartis). Heterozygous Tg-9813[A53T] $\alpha$ S mice developed a severe and fatal motor phenotype spontaneously at an early age ( $7\pm 1$  months). A score sheet with a grading scale was used to evaluate the occurrence of motor symptoms in these mice. Moreover, changes in body weight were used as clinical parameters to define the humane endpoints (i.e. loss of  $>20\%$  of the initial weight). Initially, the mice showed a disturbance in balance and gait, culminating in ataxia. As the movements became slower, tremor and rigidity were often seen. At the end-stage of the illness, partial paralysis of hind limbs occurred. With the appearance of the first clinical symptoms, mice were provided with wet food pellets in the cage. All mice were kept under specific pathogen-free conditions and maintained on a 12 h light/dark cycle with food and water *ad libitum*. The experimental procedures were undertaken in compliance with the veterinary office regulations of Baden-Württemberg (Germany) and approved by the local Animal Care and Use Committees.

## 2.2 CSF collection

CSF collection was done as described previously (Maia et al., 2015) with modifications. In short, after anesthetizing the mice with a mixture of ketamine (100 mg/kg body weight) and xylazine (10 mg/kg body weight) in saline, CSF was immediately harvested from the cisterna magna. On average, 15-20  $\mu$ l CSF were collected. CSF samples were then centrifuged at 2'000 x g for 10 min, assessed macroscopically for blood contamination, aliquoted, and stored at -80°C until further use.

## 2.3 Injection material

### 2.3.1 Brain tissue extracts

The A30P and A53T extracts were prepared from brainstems of spontaneously ill Tg-[A30P] $\alpha$ S mice (17-20 months) and Tg-9813[A53T] $\alpha$ S mice (6-8 months), respectively. After removal of the forebrain and cerebellum, the brainstems were immediately fresh-frozen on dry ice and stored at -80°C until use. Tissue was then homogenized (Precellys®24, bertin Technologies, France) to 10% (w/v) in sterile, phosphate-buffered saline (PBS, Lonza, Switzerland), vortexed and centrifuged at 3'000 x g for 5 min. The supernatant was aliquoted and immediately frozen. In addition, the A30P extract was diluted to 1:2.5 and 1:28 in PBS. Extracts were not sonicated before inoculation unless indicated otherwise. The non-tg extract was derived from aged C57BL/6J (24-26 months old). Extracts were prepared as described previously (Meyer-Luehmann et al., 2006, Eisele et al., 2009). The M83 extract was kindly provided by Dr. Thierry Baron (ANSES, Lyon Laboratory) (Mougenot et al., 2012).

### 2.3.2 Ultracentrifugation of the brain extract

Brain extracts were thawed on ice and centrifuged at 100'000 x g for 1 h at 4°C (Beckman Centrifuge). The Supernatant was then transferred to a new tube, and the intermediate fraction at the interface to the pellet was discarded. The pellet was resuspended in sterile PBS using a 1ml syringe to obtain the same volume as the supernatant. Samples were stored on ice until use. (For more details see Langer et al., 2011, Fritschi et al., 2014b)

## 2.4 Inoculations with brain extracts and CSF

Young (2-4-months-old) mice were anaesthetized with a mixture of ketamine (100 mg/kg body weight) and xylazine (10 mg/kg body weight) in saline and administered carprofen (5 mg/kg body weight) prior to surgery. Stereotactic injections were performed manually with a Hamilton syringe bilateral (2.5  $\mu$ l of brain extract/CSF per side) into the DG of the hippocampal formation (AP -2.5mm, ML  $\pm$ 2.0mm, DV -1.8mm) of homozygous Tg-[A30P] $\alpha$ S, heterozygous Tg-9813[A53T] $\alpha$ S, and homozygous Tg-M83[A53T] $\alpha$ S mice or unilateral (1  $\mu$ l) into the brainstem (AP -4.0 mm, ML +1.0 mm, DV -3.5 mm) of heterozygous Tg-[A30P] $\alpha$ S and Tg-M83[A53T] $\alpha$ S recipients. Injection speed was 1.25  $\mu$ l/min (DG) and 1  $\mu$ l/min (brainstem), respectively. The needle was kept in place for an additional 2 minutes before it was slowly withdrawn. The surgical area was cleaned with sterile saline, the incision was sutured, and the mice were monitored until recovery from anesthesia. Mice were assessed daily for routine health and checked weekly for body weight and the presence of signs of motor impairment.

## 2.5 Tissue processing

**Histology.** Mice were deeply anesthetized and transcardially perfused with ice-cold PBS for 5 min at a flow rate of 6.5 ml/min. After decapitation, the brains were removed and immersion-fixed for 48 h in 4% paraformaldehyde (EMS, Hatfield, PA, USA, in PBS, w/v), then cryoprotected in 30% sucrose (Carl Roth, Karlsruhe, Germany, in PBS, w/v) for an additional 2 days. After freezing, serial, 25  $\mu$ m-thick sagittal sections were cut through the hemisphere using a freezing-sliding microtome (SM 2000R, Leica). The sections were stored at -20°C in cryoprotection medium (25% glycerin [Applichem, Darmstadt, Germany, vol/vol] and 30% ethyleneglycol [Applichem, v/v], in PBS) until further use.

**Brain homogenates.** Fresh-frozen hemibrains of previously perfused mice were homogenized (Precellys®24) to 10% (w/v) in RIPA buffer (50 mM Tris-HCl [Sigma-Aldrich, Steinheim, Germany], 1% NP-40 [Merck Chemicals, Merck Chemicals, Darmstadt, Germany, v/v], 0.5% sodium-deoxycholate [Sigma-Aldrich, v/v], 0.1% sodium dodecyl sulfate [Sigma-Aldrich, w/v], 150 mM NaCl [Merck Chemicals], 5 mM ethylenediaminetetraacetic acid [Sigma-Aldrich], pH 8.0) with protease and phosphatase inhibitors (EDTA-free, Pierce Protease and Phosphatase Inhibitor Mini Tablets, ThermoFisher Scientific, Rockford, IL, USA), and phenylmethylsulfonyl fluoride (Sigma-Aldrich, final concentration: 1mM). Sub-

sequently, samples were centrifuged at 1'000 x g for 5 min at 4°C and the supernatant was collected, aliquoted, and stored at -80°C until use.

## 2.6 Histology

### 2.6.1 Neuropathological assessment

**IHC.** The fixed brain sections were washed with 0.1 M Tris-buffered saline (TBS, 50 mM Tris-HCl [Sigma-Aldrich], 150 mM NaCl [Merck Chemicals], pH 7.4) and mounted on microscopic glass slides (SuperFrost Plus, R. Langenbrinck, Emmendingen, Germany). After drying, the sections were treated with 0.3% H<sub>2</sub>O<sub>2</sub> (Applichem, in TBS, vol/vol) for 30 min to block the endogenous peroxidase, antigenity was enhanced by boiling the sections in 10 mM citrate buffer (1.8 mM citric acid [Applichem], 8.2 mM trisodium citrate [Applichem], pH 6.0) at 90°C for 35 min. Unspecific binding sites were blocked by using 5% normal goat serum (Invitrogen, Camarillo, CA, USA) and 0.3% Triton-X100 (Sigma-Aldrich, in TBS, vol/vol) for 30 min at RT. Rabbit monoclonal anti-pS129 (1:750, EP1536Y, Epitomics, Burlingame, CA, Germany) was applied overnight at 4°C. The sections were then incubated with biotinylated goat anti-rabbit IgG (1:400, Vector laboratories, Burlingame, CA, USA) for 45 min at RT. Antibody binding was detected by using the avidin-biotin complex system (Vector Laboratories). After avidin-biotin solution was applied for 45 min, SG Blue kit (Vector laboratories) was used as the chromogenic substrate for peroxidase. A counterstaining was performed with 0.1% nuclear fast red (Sigma-Aldrich, in distilled water, w/v) and 5% aluminium sulfate solution (Merck Chemicals, in distilled water, w/v). Lastly, the sections were then dehydrated in a series of ethanol (50% through 100%) followed by an ethanol exchange by xylene before coverslipped with Pertex mounting medium (Pertex, Medite, Burgdorf, Germany).

**Thioflavine S.** The fixed brain sections were washed with PBS and mounted on microscopic glass slides (SuperFrost Plus). After drying, the sections were incubated in 1% thioflavin S (Sigma-Aldrich, in distilled water, w/v) for 5 min, followed by a differentiation in 70% ethanol (3 x 10 min). The sections were then washed in distilled water and allowed to dry before coverslipping with Dako fluorescent mounting medium (Dako North America Inc., Carpinteria, CA, USA).

## 2.6.2 Imaging and image processing

**IHC.** Bright-field imaging of stained sections was done using a Zeiss Axioplan 2 microscope (Carl Zeiss, MicroImaging GmbH, Jena, Germany). Images were acquired with a AxioCam digital camera and a Zeiss 20X/0.5 numerical aperture (NA) objective. In addition, mosaic images were created from a series of single images acquired with a Zeiss 4X/0.1 NA objective. Axio Vision 4.8 software was used for the automated image alignment and stitching. Image editing was done using Adobe Photoshop software 12.0.4 (Adobe Photoshop CS, Berkeley, CA, USA).

**Thioflavin S.** Fluorescence imaging of stained sections was done using a Zeiss Axioplan 2 microscope with the FITC filter set (Carl Zeiss, MicroImaging GmbH, Jena, Germany). Image stacks were acquired with a AxioCam digital camera and a Zeiss 20X/0.5 NA objective (5 optical slices, 1.4  $\mu\text{m}$  thickness). Stacked images were generated using Image J software (U. S. National Institutes of Health, Bethesda, Maryland, USA). Finally, the background was corrected by applying the “rolling ball” algorithm.

## 2.7 Biochemistry

### 2.7.1 Quantification of $\alpha\text{S}$ by immunoassay

Prior to the measurement, brain homogenates and brain extracts were pretreated with formic acid (Sigma-Aldrich, final concentration: 70%), sonicated for 35 s on ice, and centrifuged at 25'000 x g for 1 h at 4°C. Supernatants were equilibrated in neutralization buffer (1 M Tris base [Sigma-Aldrich], 0.5 M  $\text{Na}_2\text{HPO}_4$  [Merck Chemicals], 0.05%  $\text{NaN}_3$  [Sigma-Aldrich, vol/vol]). In contrast, CSF samples were left untreated.

Human  $\alpha\text{S}$  was measured in brain homogenates, brain extracts, and CSF by electrochemiluminescence-linked immunoassay (Meso Scale Discovery, Gaithersburg, MD, USA). Commercial Human  $\alpha\text{S}$  Singleplex Assay was used according to the manufacturer's instructions. In brief, anti- $\alpha\text{S}$  antibody coated 96-well plates were blocked for 1 h with 1% bovine serum albumin (BSA in TBS, w/v) and washed three times with TBS. Samples were then co-incubated with the SULFO-TAG anti- $\alpha\text{S}$  detection antibody solution on the plate for 2 h. Read Buffer T (Meso Scale Discovery) was added after washing and the plate was measured immediately on the Sector Imager 6000. Data analysis was done using MSD<sup>®</sup> DISCOVERY WORKBENCH<sup>®</sup> software 2.0. All samples and calibrators were run in dupli-

cates. Samples with a coefficient of variance (CV) over 20% were excluded from the analysis or repeated if additional material was available. Internal reference samples were used as a control in every plate, and the results were adjusted for inter-plate variability.

### **2.7.2 SDS-PAGE and immunoblot analysis**

Samples were analyzed on NuPage Bis-Tris mini gels using NuPage LDS sample buffer and MES running buffer (Invitrogen, Carlsbad, CA, USA). For immunoblotting, samples were wet-blotted onto a nitrocellulose membrane, probed with anti- $\alpha$ S antibody clone 42 (BD Transduction Laboratories, Franklin Lakes, NJ, USA) and anti-human  $\alpha$ S antibody clone 15G7 (Enzo Life Sciences, Farmingdale, NY, USA). Visualization was performed with chemiluminescence using either SuperSignal West Pico (Thermo Scientific, Rockford, IL, USA) or ECL (Prime) Western Blotting Detection (GE Healthcare, Buckinghamshire, UK).

## **2.8 Statistics**

Statistical analysis was performed using GraphPad Prism 6.0 (GraphPad Software, San Diego, CA, USA). Statistical significance was assessed using one-way ANOVA followed by Tukey's post-hoc test and column statistics followed by Bonferroni's post-hoc test. Data were expressed as mean  $\pm$  SEM for the quantification of  $\alpha$ S levels. For survival analysis, log-rank test was used. Multiple comparisons of Kaplan-Meier curves were performed with Bonferroni correction. Survival curves were expressed as median incubation times (days). Statistical significance level was set as follows: \* if  $p < 0.05$ , \*\* if  $p < 0.01$ , \*\*\* if  $p < 0.001$ .

---

## 3 Results

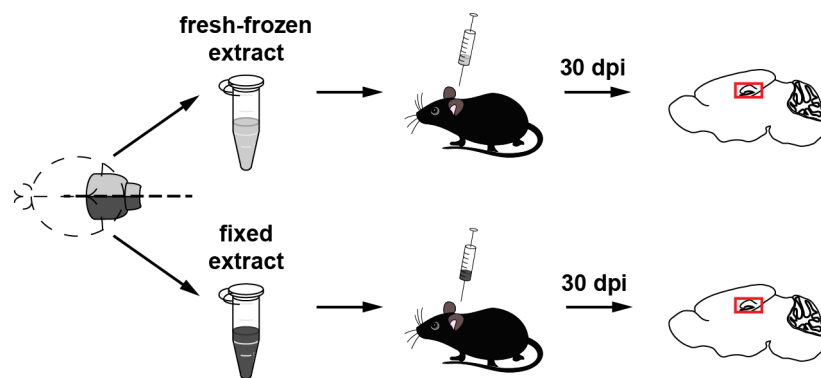
### 3.1 Seeding activity of formaldehyde-fixed $\alpha$ -synuclein pathogens

*This section is taken and/or adapted from the published manuscript (Schweighauser et al., 2015).*

Prion proteins are durable under extreme environmental conditions, which might contribute to the persistent infectivity and spread within the human body (Wiggins, 2009). Experimentally similar to prion diseases, synucleinopathy and  $\beta$ -amyloidosis can be exogenously induced by the intracerebral inoculation of brain extracts containing aggregated  $\alpha$ S or A $\beta$ , respectively, reminiscent of a prion-like seeding mechanism (Mougenot et al., 2012, Meyer-Luehmann et al., 2006). Remarkably, our lab has previously reported that extracts of formaldehyde-fixed brains from aged amyloid precursor protein (APP) tg mice or AD patients induces cerebral  $\beta$ -amyloidosis (Fritschi et al., 2014a). In contrast to A $\beta$  seed-inoculated APP tg mice, the exogenous induction of a synucleinopathy leads to an acceleration of disease and a shortening of the survival time (Mougenot et al., 2012). Given the astonishing findings of formaldehyde-resistant A $\beta$  seeds, we sought to determine whether formaldehyde-fixed tissue from aged symptomatic  $\alpha$ S tg mice would induce a fatal end-stage synucleinopathy.

#### 3.1.1 *De novo* induction of synucleinopathy with formaldehyde-fixed $\alpha$ S seeds

In a first attempt, we used Tg-9813[A53T] $\alpha$ S mice to assess the seeding capacity of formaldehyde-fixed  $\alpha$ S seeds. For that purpose, we inoculated young, pre-symptomatic mice into the DG – a brain region that lacks endogenous pathology – with extract prepared from fixed and fresh-frozen brainstem tissue (Fig. 5). As described previously, the Tg-9813[A53T] $\alpha$ S mice develop a severe and early motor phenotype spontaneously at a young age (van der Putten et al., 2000). Because of that, we sacrificed the mice after 30 days and before the appearance of the first signs of neurological dysfunction.



30-month-old Tg-9813[A53T] $\alpha$ S recipients. Mice were analyzed 30 days post-inoculation (dpi).

**Figure 5.** Schematic illustration of tissue preparation and experimental setup in Tg-9813[A53T] $\alpha$ S mice. Brainstems from a symptomatic 8-month-old tg mouse and an age-matched non-tg donor were split and each half underwent either formaldehyde fixation or was immediately fresh-frozen. Intrahippocampal injections were done in young 2- to 3-

When we examined the brains neuropathologically, deposits of phosphorylated  $\alpha$ S were found in the DG of mice inoculated with both fixed and fresh-frozen tg extracts (Fig. 6). In contrast, mice injected with fixed or fresh-frozen non-tg extract did not exhibit any phosphorylated  $\alpha$ S (pS129) inclusions. To investigate whether formaldehyde-fixed tissue is still able to induce an accelerated disease phenotype and to reproduce the results obtained in this first part, we repeated the experiment in a different mouse model of synucleinopathy.

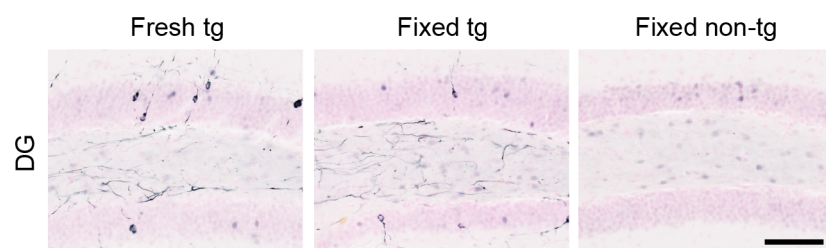


**Figure 6.** De novo induction of pathological  $\alpha$ S aggregates in the DG of Tg-9813[A53T] $\alpha$ S mice inoculated with formaldehyde-fixed brainstem tissue from a spontaneously ill donor. Immunohistochemical anal-

ysis of DG pathology at the site of injection with an antibody against S129-phosphorylated  $\alpha$ S (EP1536Y) and nuclear fast red counterstain of mice that had been injected 30 days prior with the respective extract ( $n = 2-3$  per group). Scale bar 100  $\mu$ m (applies to all panels).

### 3.1.2 Pathogenicity of fixed $\alpha$ S seeds is preserved

#### 3.1.2.1 Reduced survival after seeding by fixed $\alpha$ S seeds

Since Tg-9813[A53T] $\alpha$ S is a model of early-onset synucleinopathy, we not have been able to assess the putative differences in pathogenicity and survival between the seeding extracts. Therefore, we use additionally homozygous Tg-[A30P] $\alpha$ S mice, which do not develop a progressive deterioration of locomotor function before 1 year of age (Kahle et al., 2000a). Young, presymptomatic mice from this line were inoculated with extract from formaldehyde-fixed and fresh-frozen tg brainstem and from non-tg control tissue (Fig 7).



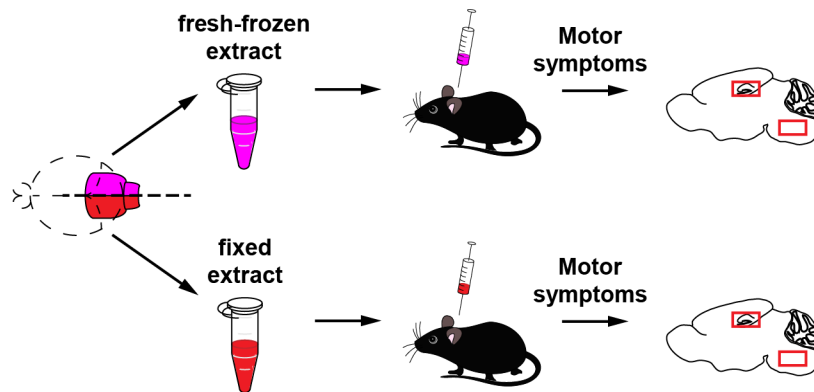


**Figure 7.** Schematic illustration of tissue preparation and experimental setup in Tg-[A30P] $\alpha$ S mice. Brainstems from a symptomatic 20-month-old tg mouse and an age-matched non-tg donor were split and each half underwent either formaldehyde fixation or was immediately fresh-frozen. Intrahippocampal injections were done in asymptomatic 4- to 6-month-old Tg-

[A30P] $\alpha$ S recipients. Mice were analyzed at the clinical end-stage displaying motor symptoms.

First, we did a biochemical analysis of the formaldehyde-fixed and fresh-frozen extracts. SDS-PAGE and subsequent  $\alpha$ S-immunoblotting of the 3'000 x g brain homogenate supernatants revealed for the fresh-frozen tg extract the expected 14 kDa monomeric  $\alpha$ S band and some higher molecular weight bands indicative for multimeric  $\alpha$ S (Fig. 8A). On the other hand, the fixed tg brainstem extract revealed primarily high molecular weight bands indicative of cross-linking due to formaldehyde fixation. Because of this issue, it was very difficult to compare and estimate the amounts of  $\alpha$ S present in both the fixed and fresh-frozen tg extracts. In contrast to our first study, all Tg-[A30P] $\alpha$ S mice developed a severe motor syndrome and were sacrificed after the occurrence of the characteristic end-stage phenotype. Remarkably, both experimental groups of Tg-[A30P] $\alpha$ S mice inoculated with extracts from fixed and fresh-frozen tg brainstem revealed a significantly reduced life span (median incubation time [days] 238 and 164, respectively) compared to uninoculated mice (500;  $p < 0.01$ , log-rank test with Bonferroni correction) (Fig. 8B). Although not statistically significant, results indicate that the extract from the fresh-frozen material is more potent in inducing end-stage synucleinopathy compared to the extract from the formaldehyde-fixed tissue.

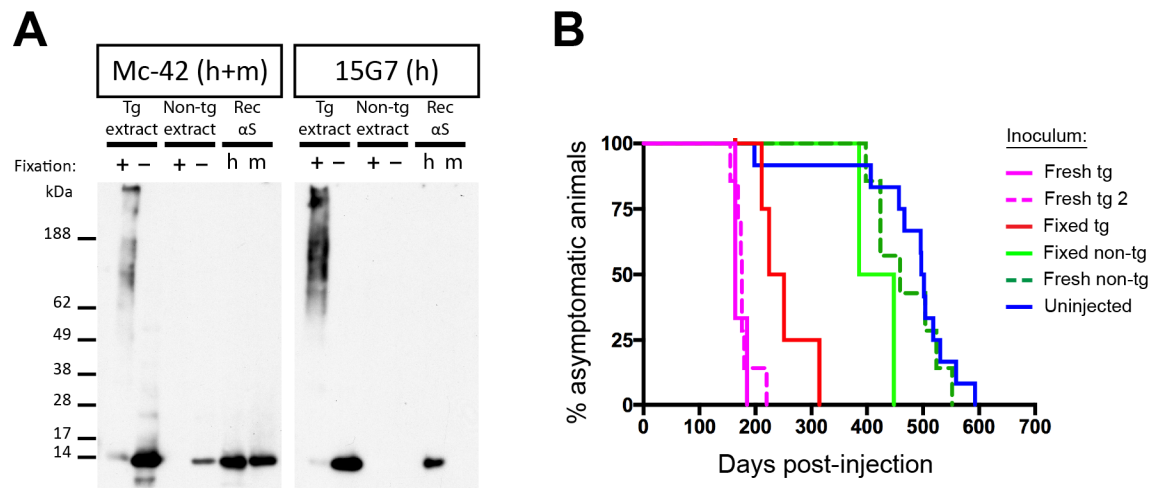


**Figure 8.** *Reduced survival in Tg-[A30P] $\alpha$ S mice after inoculation with formaldehyde-fixed brain-stem tissue from spontaneously ill donor.* **(A)** Estimation of  $\alpha$ S levels in 3'000 x g extracts of fixed and fresh-frozen brainstem tissue was done by immunoblotting. Human (h) and mouse (m)  $\alpha$ S was detected using the antibodies Mc-42 (h- and m $\alpha$ S) and 15G7 (only h $\alpha$ S). 100 ng recombinant (rec)  $\alpha$ S was loaded as control. **(B)** Kaplan-Meier curves for the appearance of clinical end-stage symptoms in Tg-[A30P] $\alpha$ S mice inoculated with extracts prepared from a fixed (red line;  $n = 4$ ) and fresh-frozen tg brainstem (purple lines;  $n = 3$  and  $n = 7$ ), a fixed non-tg brain (light green,  $n = 2$ ), and fresh-frozen non-tg brain extract (green line;  $n = 7$ ). The survival of uninoculated controls is also indicated (blue line;  $n = 12$ ).

### 3.1.2.2 Seed-induced formation of abundant synucleinopathy lesions

The assessment of the pathological state of  $\alpha$ S was done by IHC and thioflavin S labelling (Fig. 9). Perikaryal and neuritic inclusions containing phosphorylated  $\alpha$ S were observed throughout the brainstem and spinal cord of all the ill Tg-[A30P] $\alpha$ S mice reflecting the end-stage synucleinopathy (Fig. 9A, bottom panels). Furthermore, the lesions also showed intense thioflavin S labelling, indicating that these inclusions comprise proteins with  $\beta$ -sheet-rich structures (Fig. 9B, bottom row). Neuropathological examination of the DG revealed pS129-positive inclusions in the neurites and cell bodies of the granular layer of mice injected with extracts derived from formaldehyde-fixed and fresh-frozen tissue (Fig. 9A, top row). On the other hand, no immunoreactivity was observed in the DG inoculated with the extract from fixed non-tg tissue. Moreover, the lesions in the DG induced by both fixed and fresh-frozen tg extract were also found to be thioflavin S-positive demonstrating the presence of amyloid deposits in a brain region that is devoid of endogenous pathological changes (Fig. 9B, top row). When we assessed the level of induced  $\alpha$ S accumulation in the DG on blind coded sections, we found that on average the pathology (pS129 and thioflavin S) in mice injected with the fresh-frozen extract was greater compared to mice injected with the formaldehyde-fixed extract (see Table 1).

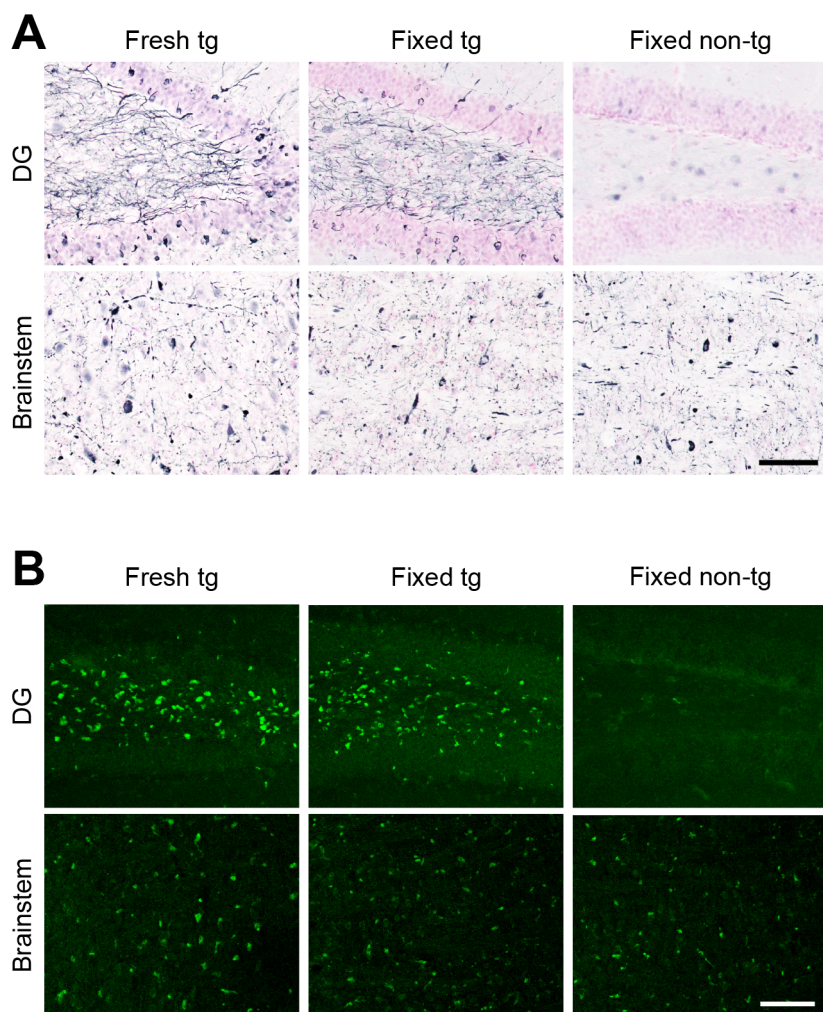


**Figure 9.** De novo induction of amyloid pathology in the DG of homozygous Tg-[A30P] $\alpha$ S mice inoculated with formaldehyde-fixed brainstem tissue from a spontaneously ill donor. (a) Immunohistochemical detection of phosphorylated  $\alpha$ S in the brains of end-stage symptomatic Tg-[A30P] $\alpha$ S mice inoculated with either fixed or fresh-frozen tg brainstem extract, as well as fixed non-tg brain extract. DG is shown in the top panels and the corresponding brainstem in the bottom panels. (b) Amyloid structure was visualised with thioflavin S. Scale bar 100  $\mu$ m (applies to all panels).

**Table 1.** Intracerebral inoculation of formaldehyde-fixed  $\alpha$ S seeds in Tg-[A30P] $\alpha$ S mice.

Inoculum	Median incubation time (days)	DG pathology*	Brainstem pathology*	Number of inoculated mice with symptoms
Fresh tg	164	+++	+++	3
Fixed tg	238	++	+++	4
Fixed non-tg	417	–	+++	2

\*Semi-quantitative pathological grading of pS129- and thioflavin S-positive labelling combined: –, none; ++, robust; +++, severe.

### 3.2 Seeding efficacy of CSF in comparison to soluble and insoluble $\alpha$ S species

Others and we have shown that extracts of fresh-frozen brain tissue from symptomatic tg mice can induce a synucleinopathy in premature tg hosts (Mougenot et al., 2012, Luk et al., 2012a, Masuda-Suzukake et al., 2013, Schweighauser et al., 2015). Following the concept of prion-like seeding, it is conceivable that the synucleinopathy-inducing factor is aggregated  $\alpha$ S. While the intercellular transfer of such protein aggregates is hypothesised to contribute to the progressive spread of Lewy pathology within the nervous system in synucleinopathies such as PD, it is still unknown which  $\alpha$ S species constitutes the seeding capacity (Recasens and Dehay, 2014). Thus, we asked ourselves whether  $\alpha$ S seeds exist outside the brain parenchyma, e.g. the cerebrospinal fluid (CSF), which could provide a possible route of transportation for such seeds. Moreover, our lab has shown earlier that soluble A $\beta$  assemblies from APP tg mice and AD brain tissue are potent A $\beta$  seeds (Langer et al., 2011, Fritschi et al., 2014b). Therefore, stimulated by the A $\beta$  findings, we wanted to know whether, and to what extent, soluble and insoluble brain-derived  $\alpha$ S is capable of inducing synucleinopathy *in vivo*.

#### 3.2.1 Quantification of brain and CSF $\alpha$ S

To study the *in vivo* seeding efficacy of CSF and soluble  $\alpha$ S from spontaneously ill synucleinopathy tg mice, we started off with the neuropathological examination and biochemical quantification of the  $\alpha$ S levels in our donor mice for both the brain-derived seeding extracts as well as the CSF.

##### 3.2.1.1 Histopathology and brain $\alpha$ S levels

First, the neuropathology and the levels of brain  $\alpha$ S were examined in a mouse model of late-onset synucleinopathy at different ages. Therefore, mice from Tg-[A30P] $\alpha$ S line served both as donors as well as hosts.

For histology, the left hemispheres of the brains from spontaneously ill Tg-[A30P] $\alpha$ S mice were stained with an antibody against pS129. The pS129-positive labelling revealed widespread  $\alpha$ S lesions in the brainstem (spinal cord, medulla, pons, midbrain) that is account-

able for the severe motor phenotype at the clinical endpoint (Fig. 10A, sagittal brain section with inserts). Conversely, young and middle-aged mice that were asymptomatic at the time of preparation showed no pS129- $\alpha$ S inclusions in the brainstem.

To determine the levels of brain  $\alpha$ S, the right hemispheres from asymptomatic and spontaneously ill mice were homogenised to 10% (w/v) in RIPA buffer. For a better comparison between the age groups, we performed a formic acid extraction prior to the measurement in order to solubilise all the  $\alpha$ S protein. The levels of total human  $\alpha$ S protein were then measured by electrochemiluminescent (ECL) immunoassay (Fig. 10B). We found that the transgenic  $\alpha$ S levels from the 3-month-old Tg-[A30P] $\alpha$ S mice (~88'000 pmol/g wet brain) were significantly lower than in the 10-11-month-old mice (~103'000 pmol/g) and the 16-19-month-old animals (~99'000 pmol/g).

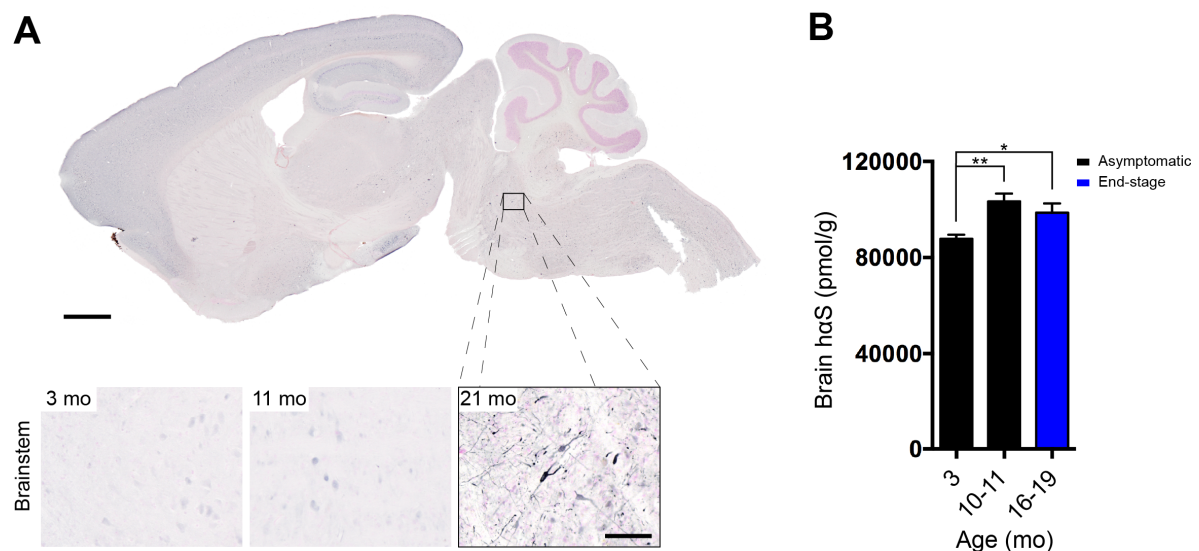


**Figure 10.** Histopathology and brain  $\alpha$ S levels in Tg-[A30P] $\alpha$ S mice at different ages. **(A)** Immunohistochemical detection of pS129  $\alpha$ S deposits in Tg-[A30P] $\alpha$ S mice. Sagittal brain section of a 21-month-old representative mouse with severe motor phenotype. For comparison, the representative images of the brainstems from a 3-month-old and a 11-month-old mouse that were devoid of the clinical symptoms are also shown. *Scale bars* 1'000  $\mu$ m (sagittal brain section) and 100  $\mu$ m (close-up image, applies to all panels). **(B)** Quantification of human (h)  $\alpha$ S levels in the brains of Tg-[A30P] $\alpha$ S mice at different ages. The brain  $\alpha$ S levels measured in animals of the youngest age group ( $n = 6$ ) were found to be significantly lower than in the other two groups ( $n = 4$  for both; ANOVA,  $F[2, 11] = 0.3674$ ,  $p < 0.01$ ). Differences between all the groups were analyzed using Bonferroni's post-hoc test for multiple comparisons. \* $p < 0.05$ , \*\* $p < 0.01$ . All data represented as group means  $\pm$  SEM.

### 3.2.1.2 Elevated levels of $\alpha$ S in the CSF of diseased mice

Next, we investigated how the levels of  $\alpha$ S in CSF from Tg-[A30P] $\alpha$ S mice change with age. Therefore, CSF from young (3 months-old) and middle-aged (10-11 months-old) mice as well as from spontaneously ill animals was harvested (18-22 months-old). Since we could not get CSF from all the mice that were used for the quantification of brain  $\alpha$ S levels, additional mice were included. Therefore, the two symptomatic age groups used for brain  $\alpha$ S and CSF  $\alpha$ S level measurement are different. The procedure of CSF collection was terminal and done as described previously (Maia et al., 2013). Remarkably, we found a dramatic increase of transgenic  $\alpha$ S in the CSF, which coincided with the presence of severe motor impairment (Fig. 11). The levels of  $\alpha$ S in 18- to 22-month-old Tg-[A30P] $\alpha$ S mice at the end-stage increased by 17-fold in comparison to both pre-mature age groups.

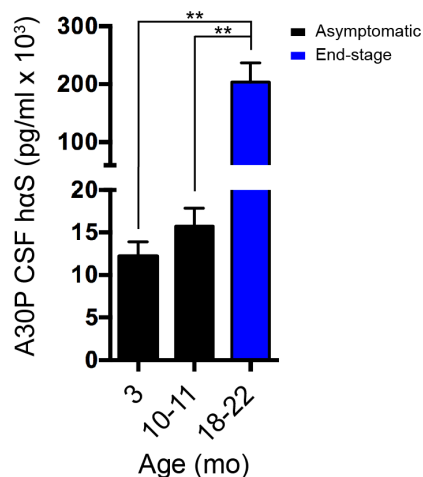
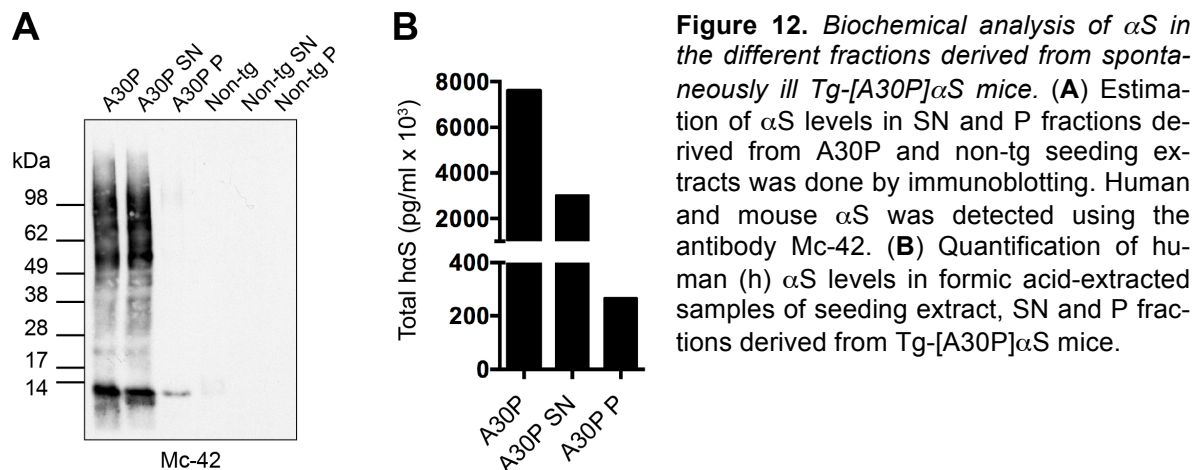


**Figure 11.** Increase of CSF  $\alpha$ S in terminally ill Tg-[A30P] $\alpha$ S mice compared to asymptomatic controls. Quantification of human (h)  $\alpha$ S levels in the CSF of Tg-[A30P] $\alpha$ S mice at different ages. In both mouse models the CSF  $\alpha$ S levels measured in animals at the clinical end-stage were significantly increased as compared to the levels measured in the CSF of asymptomatic mice ( $n = 4-8$  mice per group; means  $\pm$  SEM; ANOVA,  $F[2, 13] = 19.30$ ,  $p < 0.001$ ). Differences between the youngest and all the other age groups were analyzed using Bonferroni's post hoc test for multiple comparisons.  $**p < 0.01$ ,  $***p < 0.001$ .

### 3.2.1.3 Level of $\alpha$ S in different fractions after ultracentrifugation

Tg ("A30P") and non-tg extracts were ultracentrifuged (100'000 x g for 1 h at 4°C) and the supernatant ("SN") and pellet ("P") fractions were obtained as described (see Material and Methods). The supernatant fraction corresponds to the PBS-soluble and the pellet to the PBS-insoluble portion of the extract. SDS-PAGE and subsequent  $\alpha$ S-immunoblotting was done with samples of the supernatant and pellet fractions (Fig. 12A). In addition and for comparison, the initial 3'000 x g seeding extracts were also loaded. When comparing the monomeric  $\alpha$ S bands at 14 kDa, we found the great majority of  $\alpha$ S was in the supernatant fraction, while the pellet fraction contained only a small portion of  $\alpha$ S. For a quantitative evaluation of our inocula, we additionally measured the  $\alpha$ S protein levels of the different fractions by ECL ELISA (Fig. 12B). The results revealed that after ultracentrifugation of the

A30P seeding extract approximately 40% of  $\alpha$ S in the supernatant and less than 4% in the pellet fraction remained confirming our previous findings by immunoblot (Fig. 12A).



### 3.2.2 Lack of pathogenicity of synucleinopathy CSF and soluble $\alpha$ S *in vivo*

Given the increased levels of  $\alpha$ S in the CSF of symptomatic mice, we sought to determine whether the CSF contains  $\alpha$ S species that could induce an acceleration of the disease and a shortening of life span in tg recipients. Therefore, we performed intracerebral inoculations into the DG of young, pre-symptomatic Tg-[A30P] $\alpha$ S mice with CSF from spontaneously ill donors (Fig. 13). As a negative control, we injected the hosts with CSF from age-matched non-tg mice.

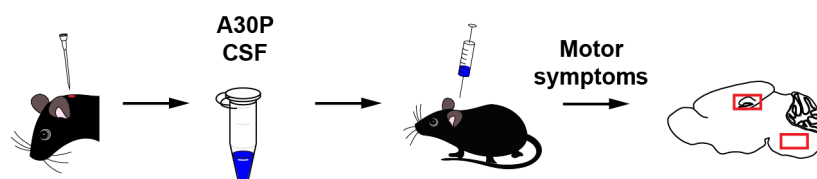


**Figure 13. Schematic illustration of experimental setup with CSF harvesting.** Intrahippocampal injections in 2-month-old pre-symptomatic Tg-[A30P] $\alpha$ S mice with Tg-[A30P] $\alpha$ S-derived (“A30P”) CSF. Mice were prepared and analyzed at clinical end-stage displaying motor symptoms.

Additionally, we wanted to investigate the synucleinopathy-inducing activity of soluble and insoluble  $\alpha$ S, since extracts derived from fresh-frozen brainstem tissue of spontaneously ill Tg-[A30P] $\alpha$ S mice contain potent seeds as shown previously. In a first attempt, the super-

natant fraction derived from A30P extract was inoculated into the DG of young, pre-symptomatic Tg-[A30P] $\alpha$ S mice (Fig. 14). As a negative control, tg mice were injected with the supernatant fraction derived from non-tg extract.



**Figure 14.** Schematic illustration of the experimental setup with the tissue preparation to extract the soluble  $\alpha$ S. The seeding extract derived from spontaneously ill Tg-[A30P] $\alpha$ S („A30P“) mice was further processed (100'000 x g for 1 h). The PBS-soluble supernatant („SN“) was then collected. Intrahippocampal inoculation was done in 2-3-month-old pre-symptomatic Tg-[A30P] $\alpha$ S mice and analyzed at clinical end-stage displaying motor symptoms.

### 3.2.2.1 No difference in incubation times after seeding

After the mice were sacrificed, we looked at the incubation times of the mice inoculated with CSF or supernatant fraction from Tg-[A30P] $\alpha$ S donors (Fig. 15). Surprisingly, synucleinopathy CSF-inoculated Tg-[A30P] $\alpha$ S mice had a median incubation period of 511 days, which was not different from non-tg-injected mice (515 days). Similarly, soluble fraction from symptomatic donor did not induce an acceleration of disease in comparison to non-tg supernatant (513 and 538 days, respectively). Furthermore, statistical analysis revealed that incubation times were not different between any of the injection groups.

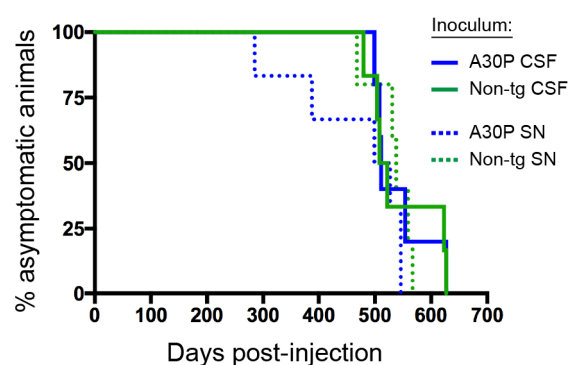


**Figure 15.** No difference in the incubation time of Tg-[A30P] $\alpha$ S mice after inoculation with CSF and PBS-soluble  $\alpha$ S from spontaneously ill donors or non-tg controls. (A) Kaplan-Meier curves for the appearance of clinical end-stage symptoms in Tg-[A30P] $\alpha$ S mice inoculated with CSF (solid lines) and 100'000 x g PBS-soluble supernatant (dotted lines; denoted as „SN“). Survival in Tg-[A30P] $\alpha$ S mice inoculated with CSF from symptomatic Tg-[A30P] $\alpha$ S mice (blue line;  $n = 6$ ) and CSF from age-matched non-tg donors (green line;  $n = 6$ ). For comparison, the SN fraction of brainstems prepared from symptomatic Tg-[A30P] $\alpha$ S mice (blue dotted line;  $n = 6$ ) and brains from non-tg wildtype mice (green dotted line;  $n = 5$ ) are shown. Multiple comparison analysis revealed that survival was not different between any of the injection groups.

Multiple comparison analysis revealed that survival was not different between any of the injection groups.



### 3.2.2.2 No induction of $\alpha$ S aggregation by CSF and soluble $\alpha$ S

Next, we assessed the histopathological seeding activity in the DG (i.e. the site of injection) of mice inoculated with either CSF or the supernatant fraction from spontaneously ill donors. Brain sections were stained with pS129-antibody and thioflavin S to reveal  $\alpha$ S lesions (Fig. 16). In addition to the DG, we also checked the level of  $\alpha$ S pathology in the brainstems from all the animals to confirm neuropathologically the observed clinical motor signs.

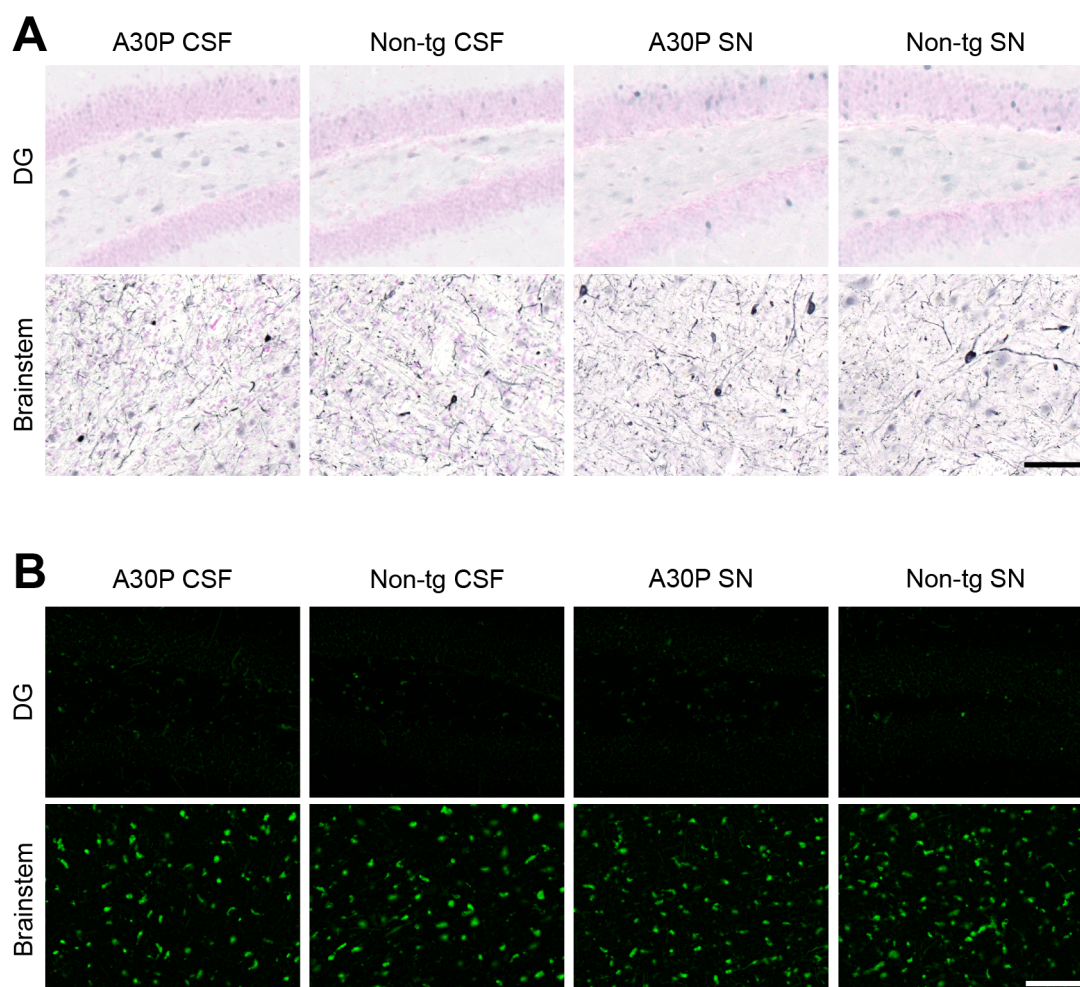


**Figure 16.** No induction of synucleinopathy in the DG of Tg-[A30P] $\alpha$ S mice inoculated with CSF or PBS-soluble  $\alpha$ S. (A) Immunohistochemical detection of pS129 in the DG and the brainstems of end-stage symptomatic Tg-[A30P] $\alpha$ S mice inoculated with CSF and 100'000 x g PBS-soluble supernatant (SN) from symptomatic tg donors and non-tg mice. Scale bar 100  $\mu$ m (applies to all panels). (B) Histological labelling of amyloids with thioflavin S in the DG and the brainstem of end-stage symptomatic Tg-[A30P] $\alpha$ S mice inoculated with CSF and SN from symptomatic tg donors and non-tg mice. Scale bar 100  $\mu$ m (applies to all panels).

None of the brains from Tg-[A30P] $\alpha$ S mice injected with A30P or non-tg CSF (aged 19-23 months and 18-23 months, respectively) induced the aggregation of  $\alpha$ S in the DG (Fig. 16, top row, first and second columns). Likewise, neither A30P nor non-tg supernatant-inoculated mice (aged 15-20 months and 18-21 months, respectively) did show neuropathological changes in the DG (Fig. 16, top row, third and fourth columns). On the other hand, widespread  $\alpha$ S pathology with similar amount of perinuclear inclusions and dystrophic neurites was observed in all the brainstems of symptomatic mice (Fig. 16, bottom rows).

**Table 2.** Summary of intracerebral inoculations with CSF and PBS-soluble  $\alpha$ S

Inoculum	Median incubation time (days)	DG pathology*	Brainstem pathology*	Number of inoculated mice with symptoms
A30P CSF	511	–	+++	5
Non-tg CSF	515	–	+++	6
A30P SN	513	–	+++	6
Non-tg SN	538	–	+++	5

\*Semi-quantitative pathological grading of pS129- and thioflavin S-positive labelling: –, none; +++, severe.

### 3.2.3 Pathological seeding properties of insoluble $\alpha$ S aggregates *in vivo*

Because of the (negative) results obtained from the CSF and soluble  $\alpha$ S seeding experiments and to further investigate the synucleinopathy-inducing factor, we then also inoculated the PBS-insoluble  $\alpha$ S fraction from terminally sick donors into young, pre-symptomatic mice (Fig. 17).

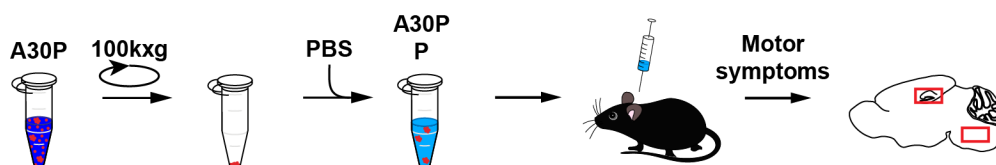


**Figure 17.** Schematic illustration of the experimental setup with extract preparation to obtain the insoluble  $\alpha$ S. A normal seeding extract (see Material and Methods) of spontaneously ill Tg-[A30P] $\alpha$ S („A30P“) mice was further processed (100'000 x g for 1 h). The Pellet („P“) was resuspended in PBS. Intrahippocampal inoculation was done in 2-4-month-old pre-symptomatic Tg-[A30P] $\alpha$ S mice and analyzed at clinical end-stage displaying motor symptoms.

To compare the seeding efficacy of our fractions, we additionally diluted the original seeding extract in PBS to match the  $\alpha$ S levels with both the supernatant and the pellet fractions (see Fig. 12). According to the ELISA measurement, we assumed a dilution of 1:2.5 for the supernatant and 1:28 for the pellet fraction. Together with the pellet fraction, we inoculated these diluted extracts into the DG of pre-symptomatic mice.

### 3.2.3.1 Reduced incubation time after seeding by insoluble $\alpha$ S seeds

After the intracerebral inoculation of pre-symptomatic Tg-[A30P] $\alpha$ S mice with the PBS-insoluble pellet fraction and the diluted seeding extracts, we analyzed the incubation times of the respective injection materials.

As expected, we found that the survival time for the  $\alpha$ S-containing insoluble fraction and the diluted seeding extracts were all significantly shorter when compared to the pellet fraction derived from non-tg brain tissue (Fig. 18). However, we found no difference between the fraction containing the insoluble  $\alpha$ S seeds and the diluted 1:28 seeding extract, whereas the median incubation time for the diluted 1:2.5 seeding extract was significantly shorter than for the 1:28.

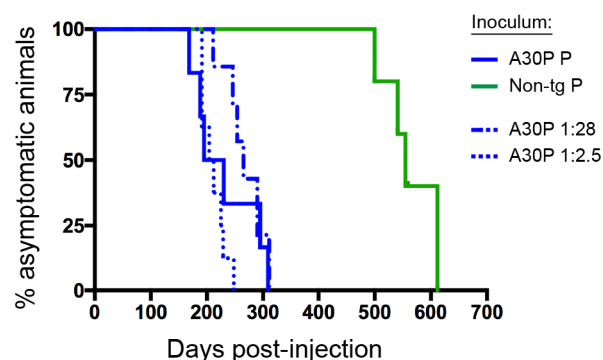


**Figure 18.** Reduced incubation times in Tg-[A30P] $\alpha$ S mice after inoculation with PBS-insoluble  $\alpha$ S. Kaplan-Meier curves for the appearance of clinical end-stage symptoms in Tg-[A30P] $\alpha$ S mice inoculated with A30P P (blue line; median incubation time [days] 212.5;  $n = 6$ ), 1:2.5 (blue dashed line; 208;  $n = 8$ ) and 1:28 (blue dotted line; 265;  $n = 7$ ) diluted A30P SE. As a control, non-tg P (green line; 555;  $n = 5$ ) is also shown.  $p < 0.01$ , log-rank test with Bonferroni correction.

### 3.2.3.2 Formation of abundant synucleinopathy lesions by insoluble $\alpha$ S seeds

When we analyzed the brains of the symptomatic Tg-[A30P] $\alpha$ S mice, we found that the PBS-insoluble fraction prepared from synucleinopathy brainstem tissue induced severe  $\alpha$ S pathology with lots of perikaryal inclusions within the DG. By contrast, the pellet fraction from control tissue did not lead to  $\alpha$ S aggregation (Fig. 19A, B, top row, first and second columns). Likewise, both diluted seeding extracts induced pS129- and thioflavin S-positive inclusions (Fig. 19A, B, top row, third and fourth columns). However, the results revealed a

dilution-dependent induction of  $\alpha$ S aggregation in the DG, whereas the seeding capacity of the insoluble  $\alpha$ S seeds appears to be increased (Table 3). As expected, widespread  $\alpha$ S pathology with similar amount of deposits around neuronal perikarya and dystrophic neurites was observed in the brainstems of all the mice.

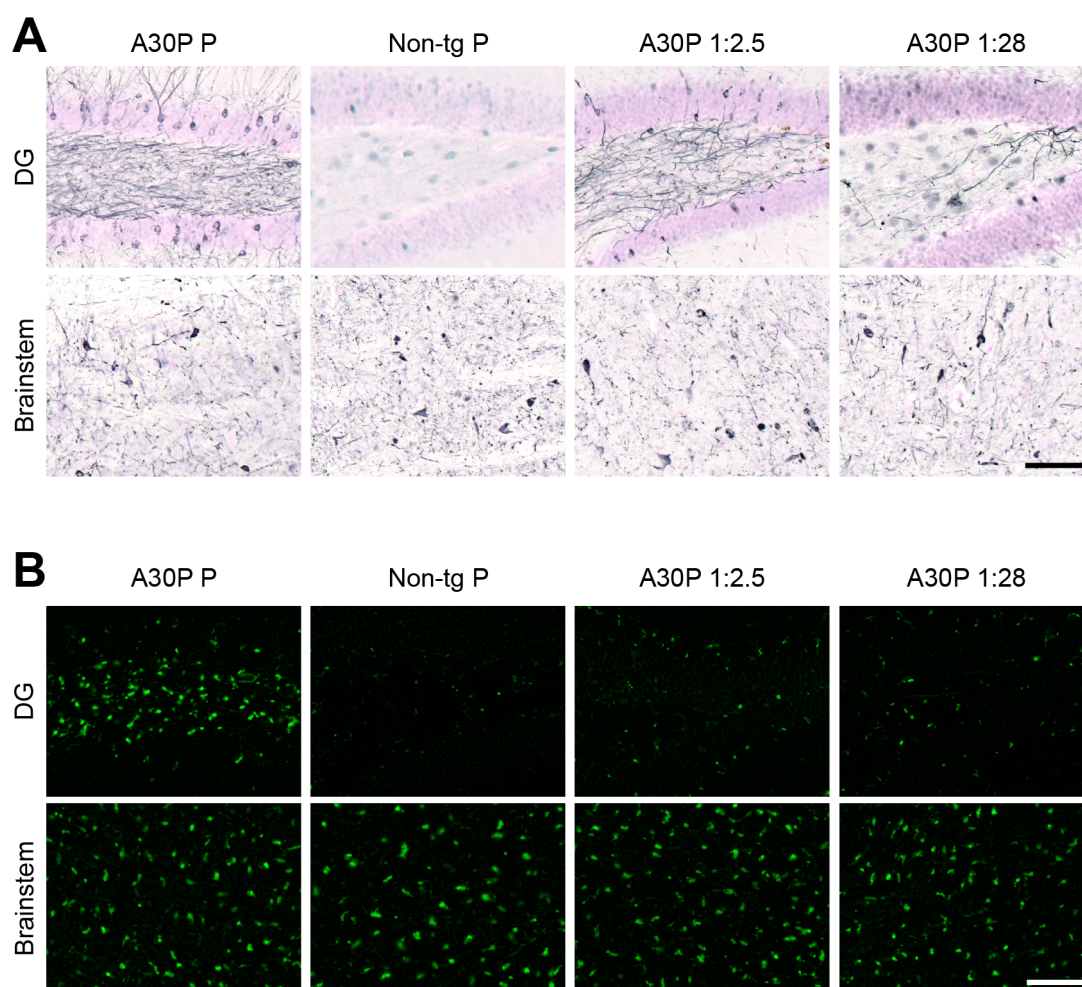


**Figure 19.** Severe induction of synucleinopathy in the DG of Tg-[A30P] $\alpha$ S mice inoculated with PBS-insoluble  $\alpha$ S. **(A)** Immunohistochemical detection of pS129 in the DG (top panels) and the brainstem (bottom panels) of end-stage symptomatic Tg-[A30P] $\alpha$ S mice inoculated with insoluble  $\alpha$ S (A30P P), 1:2.5 and 1:28 diluted seeding extract. As a control, non-tg pellet is also shown. *Scale bar* 100  $\mu$ m (applies to all panels). **(B)** Histological labelling of amyloids with thioflavin S in the DG and the brainstem of end-stage symptomatic Tg-[A30P] $\alpha$ S mice inoculated with A30P, 1:2.5 and 1:28 diluted A30P. As a control, non-tg P is also shown (see **(A)**). *Scale bar* 100  $\mu$ m (applies to all panels).

**Table 3.** Summary of intracerebral inoculations with PBS-insoluble  $\alpha$ S

Inoculum	Median incubation time (days)	DG pathology*	Brainstem pathology*	Number of inoculated mice with symptoms
A30P P	212.5	+++	+++	6
Non-tg P	555	–	+++	4
A30P 1:2.5	208	++	+++	8
A30P 1:28	265	+	+++	7

\*Semi-quantitative pathological grading of pS129- and thioflavin S-positive labelling: –, none; +, mild; ++, robust; +++, severe.

### 3.3 Cross-seeding capacities of non-homologous mutant $\alpha$ -synuclein seeds

Data from cell-free system studies suggest that mutant-type  $\alpha$ S fibrils exhibit structural and functional differences (Li et al., 2001, Yonetani et al., 2009). Therefore, we asked whether two common point mutations of the human  $\alpha$ S gene, A53T (Polymeropoulos et al., 1997) and A30P (Krüger et al., 1998), have distinct functional characteristics *in vivo*.

#### 3.3.1 Exogenous cross-seeding is influenced by host

To investigate whether mutant protein A53T and A30P  $\alpha$ S exhibit a differential induction profile, we performed a cross-seeding experiment with extracts containing either of the aggregated mutant-type  $\alpha$ S. Both mouse lines, Tg-M83[A53T] $\alpha$ S and Tg-[A30P] $\alpha$ S, are models with a delayed onset of motor symptoms and thus well suited for inoculation studies with survival time analysis. Therefore, we inoculated young presymptomatic Tg-M83[A53T] $\alpha$ S and Tg-[A30P] $\alpha$ S mice with both M83 and A30P extract (Fig. 20). Injections were done bilaterally into the DG (2.5  $\mu$ l per side).

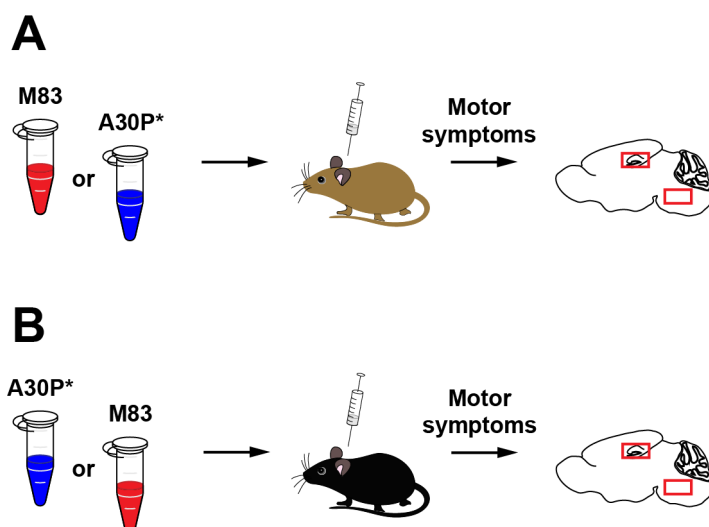


**Figure 20.** Schematic illustration of intrahippocampal inoculations in homozygous Tg-M83[A53T] $\alpha$ S and Tg-[A30P] $\alpha$ S mice. (A, B) Both extracts containing either A53T (M83) or A30P mutant  $\alpha$ S pathogens were injected into the hippocampus of 2-3-month-old presymptomatic Tg-M83[A53T] $\alpha$ S (A) or Tg-[A30P] $\alpha$ S mice (B). A30P\* extract was derived from spontaneously ill Tg-[A30P] $\alpha$ S mice (17-19 months of age) with sonication. M83 extract was kindly provided by T. Baron (Lyon, France). Mice were sacrificed after displaying motor symptoms.

### 3.3.1.1 Both hosts can be seeded by each type of mutant $\alpha$ S seed

Afterwards we incubated the mice until the occurrence of the motor symptoms. As for the previous studies, the time periods between the injections and the preparations served as readouts for the pathogenicity of the respective inoculum. We found that both  $\alpha$ S extracts reduced the incubation period significantly in both lines when compared to non-tg extract (Fig. 21A, B). Moreover, these injection groups showed uniformly shortened incubation times with low intra-group variability than mice infused with non-tg extract. In Tg-M83[A53T] $\alpha$ S mice, the median incubation time for M83 and A30P extracts were 147 days and 129.5 days, respectively (Fig 21A), whereas non-tg extract-inoculated mice had a median incubation period of 436 days ( $p < 0.017$ , log-rank test with Bonferroni correction). On the other hand, M83- and A30P-inoculated Tg-[A30P] $\alpha$ S mice had median incubation times of 203 days and 180 days, respectively (Fig. 21B). Tg-[A30P] $\alpha$ S mice infused with the non-tg control extract showed a median incubation period of 490 days ( $p < 0.017$ , log-rank test with Bonferroni correction). However, in neither of the host lines the two mutant-type  $\alpha$ S extracts revealed a significantly different incubation period from each other.

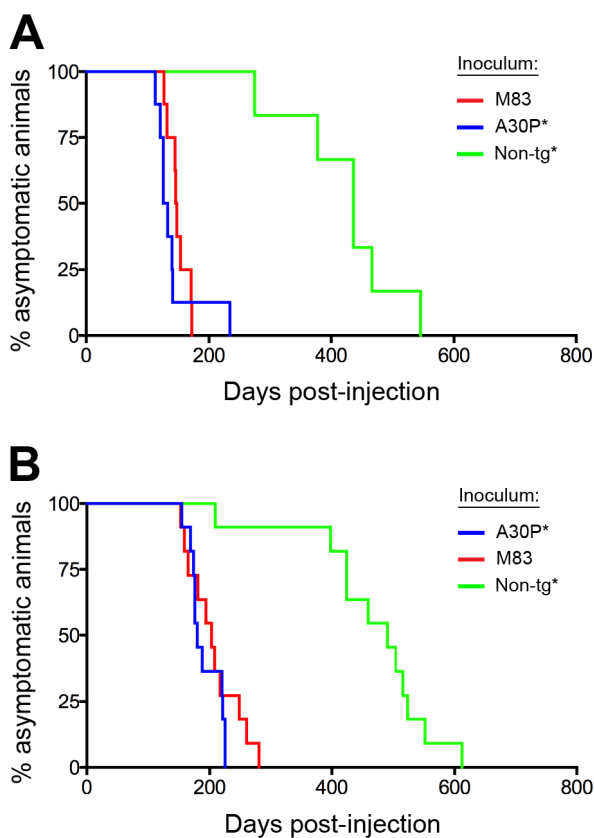


**Figure 21.** No difference in incubation period between M83 and A30P extract-injected mice. (A, B) Kaplan-Meier curves for the appearance of clinical end-stage symptoms in Tg-M83[A53T] $\alpha$ S (A) and Tg-[A30P] $\alpha$ S (B) mice inoculated with both M83- and A30P-derived extracts. (A) Survival of Tg-M83[A53T] $\alpha$ S inoculated with M83 (red line; 127-172 dpi;  $n = 8$ ), A30P (blue line; 112-234 dpi;  $n = 8$ ), and non-tg extract (green line; 275-546 dpi;  $n = 6$ ). (B) Survival of Tg-[A30P] $\alpha$ S inoculated with A30P (blue line; 155-225 dpi;  $n = 11$ ), M83 (red line; 153-281 dpi;  $n = 11$ ), and non-tg extract (green line; 203-612 dpi;  $n = 11$ ).

### 3.3.1.2 Pattern of neuropathology is predetermined by the host

To assess the level of induced pathology, we analyzed the DG of these mice. Immunolabelling of pS129 revealed both perinuclear and neuritic inclusions in the DG of Tg-M83[A53T] $\alpha$ S inoculated with M83 and A30P extract (Fig. 22A, left and center columns). In contrast, mice injected with the control extract had no induced  $\alpha$ S lesions in the DG (Fig. 22A, right column). Qualitatively, there was no difference in the level of induced pathology between the  $\alpha$ S extracts. Likewise, both M83- and A30P-inoculated Tg-[A30P] $\alpha$ S mice showed an equal level of seeded  $\alpha$ S pathology in the DG, while the control extract failed to induce pathological lesions (Fig. 22B). The brainstems of all the mice had widespread  $\alpha$ S lesions with similar amount of perikaryal and neuritic deposits (Fig. 22A, B, bottom rows).

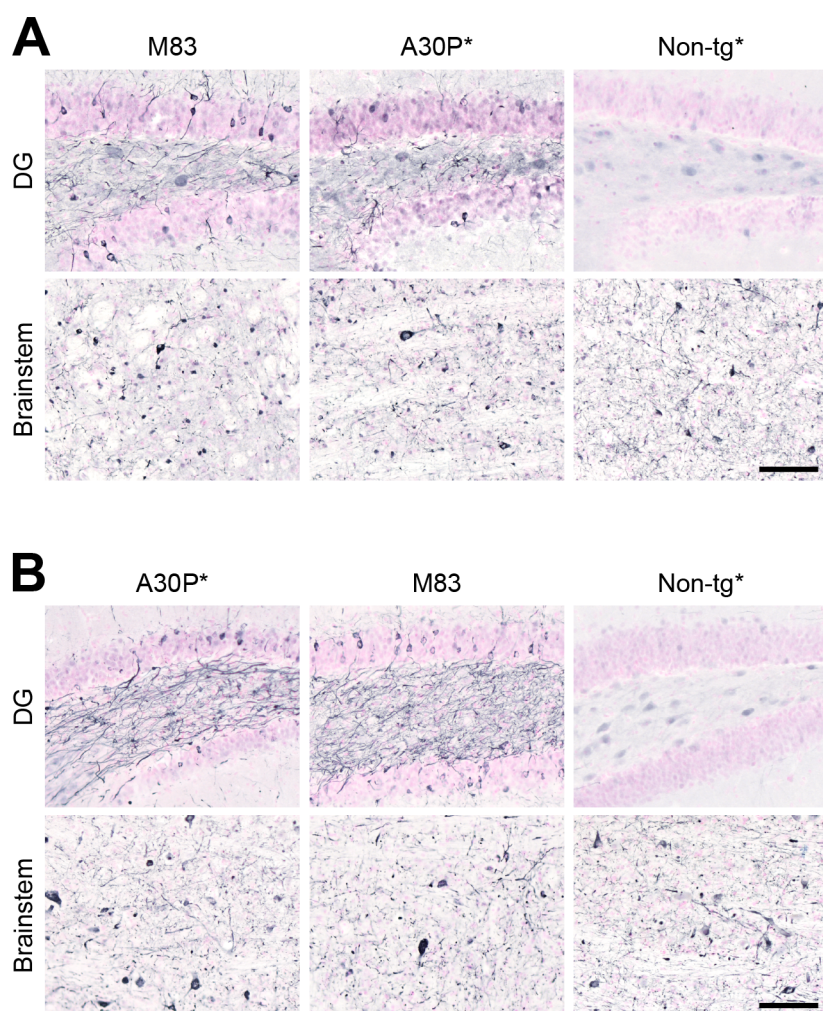


**Figure 22.** Induction of synucleinopathy lesions in the DG of both homozygous Tg-M83[A53T] $\alpha$ S and Tg-[A30P] $\alpha$ S mice. (A, B) Immunohistochemical detection of pS129 in the DGs and the brainstems of end-stage symptomatic Tg-M83[A53T] $\alpha$ S (A) and Tg-[A30P] $\alpha$ S (B) mice. (A) Tg-M83[A53T] $\alpha$ S inoculated with M83 (left column), A30P (center column), and non-tg extracts (right column). Scale bar 100  $\mu$ m (applies to all panels). (B) Tg-[A30P] $\alpha$ S inoculated with A30P (left column), M83 (center column), and non-tg extracts (right column). Scale bar 100  $\mu$ m (applies to all panels).



### 3.3.2 Differential cross-seeding efficiency is revealed in inducible hosts

Since we did not see a differential seeding effect between two  $\alpha$ S extracts in neither of the mouse lines, we decided to repeat our study in less susceptible hosts.

#### 3.3.2.1 Inducible mouse models of synucleinopathy

Both, Tg-M83[A53T] $\alpha$ S and Tg-[A30P] $\alpha$ S mice were homozygous for the transgene and developed a clinical motor phenotype spontaneously in late adult-hood. By contrast, hemizygous Tg-M83[A53T] $\alpha$ S mice express lower levels of  $\alpha$ S and do not develop a spontaneous synucleinopathy (Giasson et al., 2002, Watts et al., 2013). However, it has been recently shown that hemizygous Tg-M83[A53T] $\alpha$ S mice were susceptible and succumbed to synucleinopathy after intracerebral inoculations with brain homogenates from MSA patients and spontaneously ill mice (Watts et al., 2013). Likewise, Tg-[A30P] $\alpha$ S mice that carry the transgene hemizygously were reported to have significantly lower  $\alpha$ S levels than the homozygous mice (Neumann et al., 2002). Moreover, we found that hemizygous Tg-[A30P] $\alpha$ S mice did not develop any signs of motor dysfunction until 20 months of age and with no hyperphosphorylated  $\alpha$ S pathology (Fig. 23). In comparison, homozygous Tg-[A30P] $\alpha$ S mice from our colony have a median survival time of 569 days (Fig. 23A).

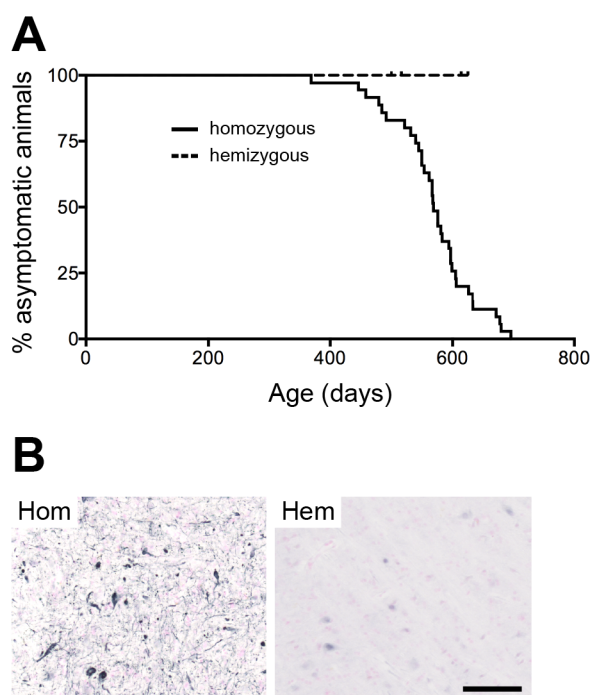


**Figure 23.** Hemizygous Tg[A30P] $\alpha$ S mice lack the endogenous  $\alpha$ S pathology. **(A)** Kaplan-Meier curve for the appearance of spontaneous end-stage symptoms in homozygous (solid line; 368-696 d; n = 35) and hemizygous (dashed line; n = 11) Tg[A30P] $\alpha$ S mice. None of the hemizygous mice had shown the clinical phenotype by the time of reporting this. **(B)** Immunohistochemical detection of pS129 in the brainstem of a spontaneously ill 19-month-old homozygous Tg[A30P] $\alpha$ S mouse and an asymptomatic 17-month-old hemizygous Tg[A30P] $\alpha$ S animal. Scale bar 100  $\mu$ m (applies to both panels).

To determine whether the two mutant-type  $\alpha$ S extracts have a differential cross-seeding capacity, we inoculated young asymptomatic Tg-M83[A53T] $\alpha$ S and Tg-[A30P] $\alpha$ S mice both carrying the transgene hemizygotously (Fig. 24). In contrast to the previous study, we injected 1 $\mu$ l of extract unilaterally into the brainstem. Moreover, we used mutant A53T  $\alpha$ S extract that derived from spontaneously ill Tg-9813[A53T] $\alpha$ S mice. The mice were sacrificed after the appearance of motor symptoms or other health issues.

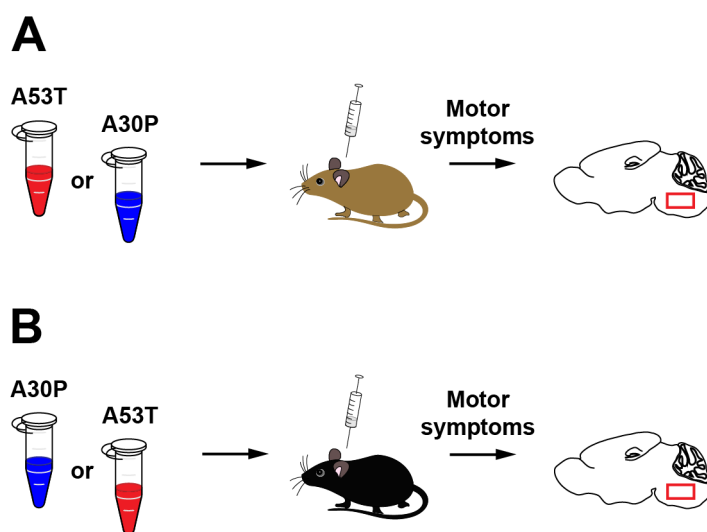


**Figure 24.** Schematic illustration of intracerebral inoculations in hemizygous Tg-M83[A53T] $\alpha$ S and Tg-[A30P] $\alpha$ S mice. (A, B) Both extracts containing either A53T or A30P mutant  $\alpha$ S pathogens were injected into the brainstems of 2-3-month-old asymptomatic Tg-M83[A53T] $\alpha$ S (A) or Tg-[A30P] $\alpha$ S mice (B). A30P extract was derived from spontaneously ill Tg-[A30P] $\alpha$ S mice (18-20 months of age). A53T extract was derived from spontaneously ill Tg-9813[A53T] $\alpha$ S (7-9 months of age). Mice were sacrificed after displaying motor symptoms.

### 3.3.2.2 Differential seeding capacities of mutant-type $\alpha$ S seeds

As previously reported by Watts and colleagues, hemizygous Tg-M83[A53T] $\alpha$ S mice inoculated with A53T extract succumbed to disease and developed motor symptoms at a median incubation time of 212 days (Fig. 25A) (Watts et al., 2013). Remarkably, the median incubation period for A30P-inoculated Tg-M83[A53T] $\alpha$ S mice was with 149 days shorter than A53T-infused mice (Fig. 25B). Although not statistically significant, it can be assumed that the A30P extract tends to be more potent than the A53T extract in hemizygous Tg-M83[A53T] $\alpha$ S mice, albeit more injections are needed to make an explicit statement. In contrast, Tg-M83[A53T] $\alpha$ S mice inoculated with the non-tg control inoculum did not show any motor impairment and were sacrificed >406 dpi. Intriguingly, all hemizygous Tg-[A30P] $\alpha$ S mice injected with mutant-type  $\alpha$ S extracts acquired the generic disease phenotype that is normally observed in homozygotes. While A30P-injected hemizygous Tg-[A30P] $\alpha$ S mice had an median incubation time of 162 days, mice infused with A53T ex-

tract developed the disease with a median incubation interval of 375 dpi. Statistical comparison of the incubation times between A30P- and A53T-extract injected mice revealed a significant difference ( $p < 0.05$ , log-rank test). By the time of reporting this study, mice inoculated with non-tg control extract were still alive (420 dpi).

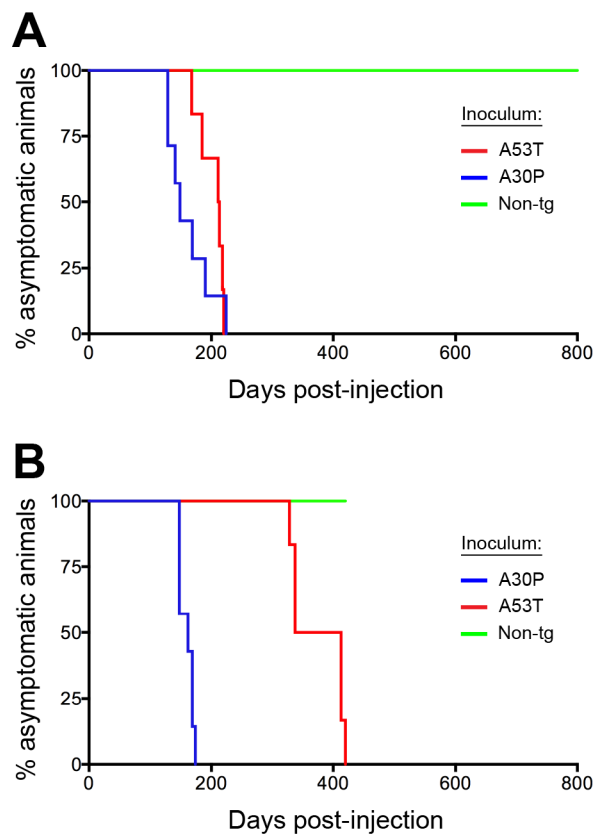


**Figure 25.** Significant difference in the incubation period between A53T and A30P extracts in hemizygous Tg-[A30P]αS mice but not in Tg-M83[A53T]αS mice. (A, B) Kaplan-Meier curves for the appearance of clinical end-stage symptoms in Tg-M83[A53T]αS (A) and Tg-[A30P]αS (B) mice inoculated with both A53T- and A30P-derived extracts. (A) Survival of hemizygous Tg-M83[A53T]αS inoculated with A53T (red line; 168-220 dpi;  $n = 6$ ), A30P (blue line; 149-224 dpi;  $n = 6$ ), and non-tg extract (green line; 406-833 dpi;  $n = 7$ ). (B) Survival of hemizygous Tg-[A30P]αS inoculated with A30P (blue line; 148-174 dpi;  $n = 6$ ), A53T (red line; 328-420 dpi;  $n = 7$ ), and non-tg extract (green line;  $n = 7$ ). At the time of reporting this study, all the mice injected with non-tg extract were still alive (420 dpi).

### 3.3.2.3 Seeded formation of *de novo* αS lesions

To investigate the level of seeded pathology in both hemizygous mouse lines, IHC against pS129 on brain sections was performed. IHC revealed widespread deposits of phosphorylated αS primarily in the brainstem of Tg-M83[A53T]αS mice inoculated with A53T extract (Fig. 26A). This was in line with previous observation by Watts and colleagues (Watts et al., 2013). Similarly, mice injected with A30P extract showed pronounced αS pathology in the brainstem (Fig. 26B). Differences in the neuropathological pattern were not immediately apparent between A53T extract injected mice and hosts that received A30P extract. In contrast, no pS129-positive pathology was observed in Tg-M83[A53T]αS mice inoculated with non-tg extract. Likewise, the brainstems of hemizygous Tg-[A30P]αS mice inoculated

with both mutant-type  $\alpha$ S extracts revealed abundant phosphorylated  $\alpha$ S lesions. At the time of writing this thesis, none of the mice injected with the control inoculum had been prepared.

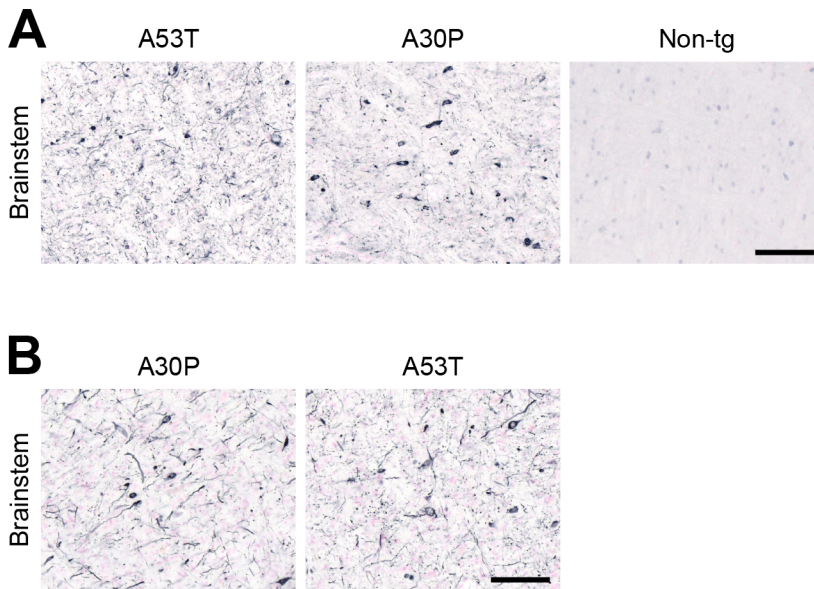


**Figure 26.** Induction of  $\alpha$ S lesions in the brainstem of both hemizygous *Tg-M83[A53T] $\alpha$ S* and *Tg-[A30P] $\alpha$ S* mice. (A, B) Immunohistochemical detection of pS129 in brainstems of end-stage symptomatic or aged hemizygous *Tg-M83[A53T] $\alpha$ S* (A) and *Tg-[A30P] $\alpha$ S* (B) mice. (A) Hemizygous *Tg-M83[A53T] $\alpha$ S* inoculated with A53T (left panel), A30P (center panel), and non-tg extracts (right panel). Scale bar 100  $\mu$ m (applies to all panels). (B) Hemizygous *Tg-[A30P] $\alpha$ S* inoculated with A30P (left panel) and A53T (right panel). Scale bar 100  $\mu$ m (applies to both panels).

## 4 Discussion

Despite decades of extensive research, there is currently still no cure for PD that affects an estimated seven to 10 million people worldwide ([www.pdf.org](http://www.pdf.org)). Besides PD,  $\alpha$ S aggregates are characteristic for e.g. DLB and MSA; hence these diseases are commonly referred to as synucleinopathies. The progressive neurodegeneration is thought to be a result of the accumulation of misfolded  $\alpha$ S within neurons or glial cells, while the cause for it remains elusive (Uversky, 2008). It is important, therefore, to understand the molecular basis of synucleinopathy pathogenesis to aid diagnosis and treatment. Recent reports, however, brought the prion concept into play to explain the underlying mechanism of the formation and propagation of pathogenic  $\alpha$ S aggregates (Goedert, 2015, Walker and Jucker, 2015). Indeed, a prion-like acceleration of synucleinopathy has been described in transgenic mice following the intracerebral inoculation with brain homogenates from symptomatic mice (Mougenot et al., 2012, Luk et al., 2012a) and synthetic fibrils (Luk et al., 2012b).

Stimulated by these findings, we aimed to further investigate the seeding properties of  $\alpha$ S species. Therefore, we performed a series of inoculation experiments using different tg mice as both hosts and donors. In contrast to other research groups, we performed the inoculations into the hippocampus (unless otherwise stated), a brain region that lacks endogenous pathology, is well-defined, and therefore easy to target (see Meyer-Luehmann et al., 2006). Moreover, it has been reported before that this region is susceptible to form  $\alpha$ S aggregates upon injection with recombinant  $\alpha$ S fibrils (Luk et al., 2012b).

The results from our work addressed three major aspects: (1) we provide evidence for the durability of  $\alpha$ S seeds with features reminiscent of prions; (2) we show that extracellular  $\alpha$ S in CSF lacks *in vivo* seeding capacity, whereas insoluble brain  $\alpha$ S is highly pathogenic; and (3) we present first indications for cross-seeding by PD-linked  $\alpha$ S mutants with non-homologous sequences.

### 4.1 Formaldehyde resistant $\alpha$ -synuclein seeds

Several studies have shown that prions are durable under extreme environmental conditions (Wiggins, 2009). For instance, the infectivity of prions is retained even after formaldehyde treatment (Pattison et al., 1965, Brown et al., 1986, Zobeley et al., 1999, Flechsig

et al., 2001). Moreover, the unusual resistance to conventional disinfection procedures may contribute to their persistent infectivity (Brown et al., 1990, Taylor et al., 1994, Taylor, 2000, Sutton et al., 2006). Likewise, it has been previously reported that prion diseases may in fact be transmitted via contaminated medical instruments during surgical procedures (Brown et al., 2000, Hamaguchi et al., 2009, Thomas et al., 2013). However, improvements in the sterilization methods have led to a substantial prevention of iatrogenic transmission (Brown et al., 2012).

Given the growing body of evidence suggesting a prion-like mechanism underlying neurodegenerative diseases such as PD or AD, concerns have been raised that iatrogenic transmission of pathological proteins other than prions may be possible. Therefore, we sought to determine whether  $\alpha$ S seeds in brain resist the fixation by formaldehyde similar to prions (Schweighauser et al., 2015). Our lab has recently demonstrated that extracts from formaldehyde-fixed brain tissue containing aggregated A $\beta$  from APP-tg mice or from AD patients retained the capacity to seed the induction of A $\beta$  deposition when injected into the brains of APP-tg hosts (Fritschi et al., 2014a). Accordingly, we performed inoculations of formaldehyde-fixed brainstem tissue extracts of symptomatic mice into heterozygous mice transgenic for A53T  $\alpha$ S under the control of the mouse Thy1 promoter (Tg-9813[A53T] $\alpha$ S) (Schweighauser et al., 2015). Intrahippocampal injections led to the formation of  $\alpha$ S inclusions in the DG after 30 days. This was true for both fixed and fresh-frozen tissue from symptomatic donors.

Seeing a seeded induction of *de novo* pathology in the DG of Tg-9813[A53T] $\alpha$ S, we next assessed if formaldehyde-fixed brain tissue from spontaneously ill mice would induce fatal end-stage synucleinopathy. Therefore, we decided to use homozygous mice transgenic for A30P  $\alpha$ S under the control of the mouse Thy1 promoter (Tg-[A30P] $\alpha$ S), because they develop a progressive and terminal motor phenotype in late adulthood (Kahle et al., 2000a, Neumann et al., 2002). We demonstrated that also in Tg-[A30P] $\alpha$ S seeded  $\alpha$ S aggregation occurred following the inoculation with formaldehyde-fixed tissue, albeit with a reduced seeding capacity in comparison to fresh-frozen tissue. Moreover, we observed an acceleration of disease in Tg-[A30P] $\alpha$ S inoculated with formaldehyde-fixed tissue. Although a tendency towards a more potent acceleration of end-stage synucleinopathy in fresh-frozen extract-infused mice could be seen, no significant differences were observed between the incubation times of mice injected with extracts from fresh-frozen and fixed-frozen material.

---

In accordance with previous studies on A $\beta$ , formaldehyde-fixed brain tissue from APP-tg donors had also a reduced seeding capacity compared to unfixed tissue (Fritschi et al., 2014a). The decreased seeding activity of fixed tissue in comparison to fresh-frozen tissue might be a cause of a reduction in the number of seeds available due to the fixation by formaldehyde. Indeed, the immunoblot analysis revealed primarily multimeric  $\alpha$ S species in the fixed tissue indicative of cross-linking due to fixation. Moreover, we followed a standardized protocol for short-term fixation (48h) that is commonly used in histology. Therefore, it is conceivable that a prolongation of formaldehyde treatment would further diminish the seeding efficacy of fixed tissue, albeit to be proven. Studies already highlighted the seeding potential of fresh-frozen human brain material from for instance DLB (Masuda-Suzukake et al., 2013) and MSA (Watts et al., 2013) patients. Therefore, a next step could be to assess the putative seeding activity of formaldehyde-fixed human brain tissue from synucleinopathy patients as it has already been shown for fixed AD brains (Fritschi et al., 2014a). Ultimately, archived formalin-fixed brain material could be exploited to further establish the relationship between the molecular architecture of  $\alpha$ S lesions and individual pathogenesis.

Taken together, the resistance to inactivation by formaldehyde underpins the persistent nature of  $\alpha$ S seeds, which may contribute to the durability and spread within the human body. Although  $\alpha$ S seeds share this remarkable feature with prion proteins, PD is not known to be contagious (Beekes et al., 2014). In contrast to prions, conventional methods for decontamination of medical devices or laboratory materials is sufficient (Thomzig et al., 2014, Bousset et al., 2016). However,  $\alpha$ S seeds are not innocuous and our results indicate that relevant precautionary measure should be taken when handling with formaldehyde fixed tissue.

#### **4.2. Lack of seeding activity in synucleinopathy CSF**

To diagnose a synucleinopathy at an early stage is very challenging. Molecular disease biomarkers in bodily fluids such as cerebrospinal fluid (CSF) or blood that reflect the pathological state in the brain could, therefore, offer valuable tools in the clinical investigation of a disease (Delenclos et al., 2016). For instance, in a study reported in *Neuron* our lab has shown that neurofilament light chain (NfL) is increased in CSF (and blood), of mouse models of synucleinopathy (among others), whereby the NfL levels also responded to the experimental induction of synucleinopathy (Bacioglu et al., 2016). Therefore, NfL in

---

CSF may serve as a biomarker to monitor disease progression in at least such mouse models. Similar to NfL, extracellular  $\alpha$ S has been investigated as a potential diagnostic biomarker for PD and related synucleinopathies, especially in the CSF (Gao et al., 2015). In the study presented here, we addressed whether CSF from mice with synucleinopathy contains pathogenic  $\alpha$ S species. In this part of the thesis, we first found elevated levels of  $\alpha$ S in the CSF of Tg-[A30P] $\alpha$ S mice, a model of late-onset synucleinopathy. Similarly to NfL, the increase in CSF  $\alpha$ S coincided with the occurrence of clinicopathological features of synucleinopathy, while the CSF levels were unchanged in the asymptomatic states. Moreover, we found an increase in CSF  $\alpha$ S after the exogenous induction of  $\alpha$ S lesions in premature tg mice (data not shown). For NfL, the increase in CSF is thought to be a result of axonal damage associated with  $\alpha$ S pathology in the spinal cord (Bacioglu et al., 2016). Likewise, in Tg-[A30P] $\alpha$ S neurodegeneration has been described to occur throughout the spinal cord (Neumann et al., 2002). Therefore, it is conceivable that elevated levels of CSF  $\alpha$ S (like NfL) might be due to secondary impacts on spinal cord neurons, even though this remains to be shown.

Seeing an increase in CSF  $\alpha$ S levels, we next sought to assess the *in vivo* seeding efficacy of CSF. However, inoculation studies revealed no seeding activity of CSF from spontaneously ill Tg-[A30P] $\alpha$ S mice or non-tg controls. One reason for this could be the comparable low concentrations of  $\alpha$ S in the CSF. A reference seeding extract contains approximately 40 times more transgenic  $\alpha$ S than CSF from spontaneously ill mice. A further reason may also be found in the sensitivity of our *in vivo* seeding assay, which might fail to detect putative seeds at such low concentrations. However, this is contradicted by preliminary data which indicate that 55-fold diluted seeding extract derived from brains of spontaneously ill donors was still able to induce synucleinopathy, albeit with reduced seeding capacity (not shown). In a study published by our group, CSF from both APP-tg mice and AD patients also failed to induce amyloid deposition, even though the total A $\beta$  concentration was orders of magnitude greater than the estimated titer (Fritschi et al., 2014b). We can only speculate, for instance, that protease digestion of  $\alpha$ S in CSF may reduce the seeding effect to such an extent that the activity is abolished. In line with our findings, a recent study also provided evidence that extracellular  $\alpha$ S is present in the CNS *in vivo* (Danzer et al., 2012). Furthermore, it has been shown that CSF exosomal  $\alpha$ S species from patients with PD and DLB induced oligomerization of  $\alpha$ S *in vitro* (Stuendl et al., 2016). However, it would be interesting to know, whether these isolated exosomal  $\alpha$ S species also confer seeding activity in animal models. Conversely, it might be worthwhile to test



the seeding potential of mouse-derived synucleinopathy CSF in an *in vitro* assay to circumvent the problem of sensitivity. Thus, further experiments are needed before final conclusion about the seeding capacity of CSF  $\alpha$ S can be drawn.

In order to define whether soluble  $\alpha$ S species is seeding active, we additionally inoculated the 100'000 x g supernatant fraction of brain-derived seeding extracts (according to Langer et al., 2011). Quantification of the transgenic  $\alpha$ S levels prior to the injection revealed a 2.5-fold difference between the initial tg seeding extract and the supernatant fraction (equal to 40% of total  $\alpha$ S). Similar to CSF, we found that both PBS-soluble fractions derived from tg or non-tg extracts failed to induce  $\alpha$ S lesions. To exclude the possibility that the lower amount of  $\alpha$ S in the soluble fraction was responsible for the negative result, we also assessed the seeding capacity of 1:2.5 diluted seeding extract. By contrast, we found that the diluted extract induced an accelerated disease phenotype with robust  $\alpha$ S deposition. Taken together, these results suggest that the PBS-soluble fraction of a brain-derived seeding extract lacks an *in vivo* seeding activity, which cannot be explained by the lower concentration of transgenic  $\alpha$ S present in this fraction. In contrast to  $\alpha$ S, previous findings from our lab revealed that the  $\beta$ -amyloid-inducing factor is partially soluble (Langer et al., 2011). Moreover, soluble A $\beta$  assemblies in brain extracts were found to be disproportionately highly potent in inducing  $\beta$ -amyloidosis. And to a further extent, a more recent study could demonstrate that the soluble AD brain fraction contains highly active A $\beta$  seeds (Fritschi et al., 2014b). Thus, these findings highlight some remarkable differences between two proteopathic particles.

Apart from the supernatant fractions, we also collected the pellets after the 100'000 x g centrifugation of tg and non-tg seeding extracts, which then were recovered by resuspension in PBS to match the volume of the supernatants. ELISA measurements of the tg pellet fraction revealed a concentration of  $\alpha$ S that was 28 times lower than in the initial seeding extract, which corresponds to less than 4% of total  $\alpha$ S. One point worthy of note, however, is the loss of  $\alpha$ S after the ultracentrifugation. As a matter of fact, less than 50% of total  $\alpha$ S remained together in the supernatant and pellet fractions. The reason for this might be the procedure of retrieving both fractions. In order to not "contaminate" the soluble fraction with pellet, the supernatant was not collected entirely leaving a small volume behind. This remaining supernatant at the interface was then collected and discarded whereby some of the pellet was included. However, this procedure ensured us to end up with "clean" fractions.

---

Given the inert seeding activity of PBS-soluble  $\alpha$ S, we asked whether and to what extent insoluble  $\alpha$ S is capable of inducing synucleinopathy in tg mice despite the low amounts of  $\alpha$ S. Strikingly, we found that insoluble  $\alpha$ S derived from tg seeding extract induced pronounced  $\alpha$ S lesions. Moreover, mice injected with the pellet fraction showed a reduced survival time compared to control injected animals. For comparison, we additionally infused mice with seeding extract that was diluted 1:28 in PBS to match with the amounts of  $\alpha$ S present in the insoluble fraction. Results revealed for the 1:28 diluted extract a mild induction of synucleinopathy with a reduced incubation time that was less prominent than in pellet-inoculated mice. These data suggest that brain-derived PBS-insoluble  $\alpha$ S from spontaneously ill mice contains seeding active species and is in line with two recent studies (Masuda-Suzukake et al., 2013, Recasens et al., 2014a). In one study from 2013, researchers assessed whether inoculation of insoluble  $\alpha$ S from brains with DLB can induce  $\alpha$ S pathology in wt mice (Masuda-Suzukake et al., 2013). Most strikingly, DLB-derived sarkosyl-insoluble  $\alpha$ S induced synucleinopathy lesions in 50% of the recipients. Moreover, mice injected with recombinant  $\alpha$ S fibrils developed abundant Lewy-like pathology, whereas mice infused with soluble  $\alpha$ S did not. A second study demonstrated that mice inoculated with PD-derived LB-enriched fractions displayed neuronal  $\alpha$ S inclusions. While on the other hand, in control animals that received non-LB fractions from the same patients, there was no pathological change apparent (Recasens et al., 2014a). In contrast, however, a recent publication demonstrated that intracerebral inoculation of both fractions of human LBD brain homogenate induced disease-associated deposits in CNS of mice (Jones et al., 2015). The authors assume that the addition of protease inhibitor preserved the seeding capacity of the soluble fraction since soluble  $\alpha$ S is more vulnerable to protease digestion than insoluble  $\alpha$ S. However, it remains to be shown how far this would relate to our brain-derived soluble fraction.

When we compared the 1:2.5 and 1:28 diluted extracts we found a concentration-dependent decrease in seeding efficiency. Moreover, the analysis of an additional dilution (1:55) is ongoing. However, further inoculations of diluted seeding extracts are needed to find conclusive evidence. Moreover, it would be of great interest to know the highest dilution factor that is still able to induce synucleinopathy. For instance, the *in vivo* end-point dilution titration is a traditional method in prion research that could be used in mice to obtain a quantitative estimate of the  $\alpha$ S pathogenicity titer (see Prusiner et al., 1982b).

---

In summary, these results revealed some interesting characteristics of pathological  $\alpha$ S. Our data indicate that extracellular  $\alpha$ S in CSF from synucleinopathy mice lacks *in vivo* seeding activity. In line with this,  $\alpha$ S pathogenicity is primarily mediated by insoluble seeds and not by soluble  $\alpha$ S. Thus, CSF  $\alpha$ S *per se* might not be suited for the use as a diagnostic marker of disease progression.

### 4.3. Cross-seeding by Parkinson's disease linked $\alpha$ -synuclein mutants

Recently, it has been hypothesized that  $\alpha$ S may behave as 'strains' with distinct biochemical and functional properties, providing an explanation for the diverse clinical phenotypes observed between the synucleinopathies in humans (Melki, 2015, Prusiner et al., 2015, Peelaerts and Baekelandt, 2016). Indeed, *in vitro* generated  $\alpha$ S fibrils exhibit structural and functional characteristics, which can even be propagated in cell culture (Guo et al., 2013, Woerman et al., 2015) or *in vivo* (Peelaerts et al., 2015). However, the different  $\alpha$ S 'strains' were generated under various solution conditions (Bousset et al., 2013, Peelaerts et al., 2015) or through repetitive seeded fibrillization *in vitro* (Guo et al., 2013).

In this part of the thesis, we focused on two common point mutations (A53T and A30P) in the  $\alpha$ S gene that have been linked to early-onset FPD (Polymeropoulos et al., 1997, Krüger et al., 1998). The folding and aggregation of these mutant-type  $\alpha$ S variants has been investigated in multiple *in vitro* studies (Conway et al., 1998, Conway et al., 2000a, Conway et al., 2000b, Li et al., 2001, Li et al., 2002, Bertoncini et al., 2005, Yonetani et al., 2009).

To investigate the functional consequences of mutant A53T and A30P human  $\alpha$ S *in vivo*, we performed two sets of cross-seeding experiments. In the first set, we used extracts of A53T  $\alpha$ S derived from spontaneously ill Tg-M83[A53T] $\alpha$ S mice ("M83"; generously provided by T. Baron, see Mougénot et al., 2012) and extracts of A30P  $\alpha$ S prepared from brain-stems of symptomatic Tg-[A30P] $\alpha$ S mice. Intrahippocampal inoculations revealed that both extracts led to an accelerated disease phenotype together with the formation of pathological  $\alpha$ S in the DG of homozygous Tg-M83[A53T] $\alpha$ S and Tg-[A30P] $\alpha$ S mice. Remarkably, both groups of M83- and A30P-inoculated mice had low incubation time variability in contrast to non-tg extract-injected recipients. This is in line with previous observations from other research groups (Mougénot et al., 2012, Watts et al., 2013). The histopathological changes in the DG were not perceptibly different between M83- and A30P-infused

---

mice of both lines. In contrast, it appeared that both hosts exerted a determinant part regarding the non-homologous cross-seeding in the corresponding recipient (i.e. A30P in Tg-M83[A53T] $\alpha$ S and M83 in Tg-[A30P] $\alpha$ S). In fact, the high expression levels of transgenic  $\alpha$ S in homozygous Tg-M83[A53T] $\alpha$ S and Tg-[A30P] $\alpha$ S mice results in a severe and progressive motor phenotype that occurs independent of an exogenous seeding event. Since the (cross-) seeding appeared to be equally efficient regardless of a sequence homology between seed and monomeric protein, we speculate that this might be due to the high abundance of transgenic  $\alpha$ S in the recipient mice.

To test this hypothesis, we repeated the experiment but this time with hemizygous Tg-M83[A53T] $\alpha$ S and Tg-[A30P] $\alpha$ S mice. The levels of overexpression in both hemizygotes were reported to be about half the levels of the regarding homozygous Tg-M83[A53T] $\alpha$ S and Tg-[A30P] $\alpha$ S mice (Giasson et al., 2002, Neumann et al., 2002), whereby hemizygotes from both lines do not spontaneously develop a neurological disease. Consequently, the inoculations were done directly into the brainstem.

Our inoculation experiment showed that both mutant-type  $\alpha$ S variants (A53T and A30P) were able to seed the induction of synucleinopathy in both hosts regardless of the genotype. Most strikingly, inoculation with A53T and A30P  $\alpha$ S revealed differential seeding characteristics in both hosts. When cross-seeded with A30P  $\alpha$ S, Tg-M83[A53T] $\alpha$ S mice succumbed to disease earlier than by homologous seeding with A53T. Although the difference was not significant, it is still a remarkable outcome. These findings are intriguing for two reasons. Firstly, the results presented here demonstrated that A30P was capable of seeding A53T  $\alpha$ S despite the sequence dissimilarity. This is all the more astonishing because it is known from prion research that a single amino acid alteration can have dramatic effects on the incubation times for instance (Manson et al., 1999). Secondly, *in vitro* studies demonstrated that A30P seeds accelerated the fibrilization of monomeric wt  $\alpha$ S more effectively than A53T fibrils (Yonetani et al., 2009), although in absence of seeds the fibrillization of monomeric A53T occurred faster than A30P (Conway et al., 1998, Yonetani et al., 2009). In line with this, our findings indicate that aggregated A30P has a strong cross-seeding effect on soluble A53T *in vivo*.

The induction of synucleinopathy in hemizygous Tg-[A30P] $\alpha$ S mice by inoculation with A30P occurred rapidly, whereas cross-seeding with A53T significantly prolonged the disease incubation period. This was consistent with our previous finding, according to which A30P is a better seed than A53T. On the other hand, this observation could also suggest

---

that Tg-[A30P] $\alpha$ S mice provide a hostile environment for A53T mutant  $\alpha$ S. Since the A30P mutation in human  $\alpha$ S has been reported to accelerate oligomerization *in vitro* (Conway et al., 2000b), we can speculate, albeit to be proven, that A53T seeds encounter an increased number of oligomeric A30P that could impede further aggregation by A53T.

While our experiments demonstrated the functional consequences of two mutant  $\alpha$ S pathogens *in vivo*, it yet remains to be shown whether these two forms of  $\alpha$ S fulfill the molecular criteria to be identified as two 'strains'. Therefore, experiments are ongoing to structurally characterize aggregated A53T and A30P  $\alpha$ S using novel conformation-sensitive dyes (described in Aslund et al., 2009). Moreover, the resistance to proteinase K digestion of both aggregates will help to assign a biochemical fingerprint to these  $\alpha$ S aggregates (Aguzzi et al., 2007, Kuczius and Groschup, 1999, Parchi et al., 1996). And ultimately, the aim is to assess whether such conformational and biochemical characteristics are propagated in a non-homologous host, which could provide evidence for templated conversion by exogenous seeds.

Taken together, our findings indicate altered seeding characteristics of PD-associated  $\alpha$ S mutants *in vivo*. We also showed that the level of transgenic overexpression in hosts might play a superordinate role for the (cross-) seeding efficacy. While it had been demonstrated earlier that in hemizygous Tg-M83[A53T] $\alpha$ S a disease can be induced by intracerebral inoculation with brain homogenates from either tg mice or MSA patients (Watts et al., 2013), it was unclear whether hemizygous Tg-[A30P] $\alpha$ S mice would be susceptible to the initiation of a neurological illness. We showed that hemizygous Tg-[A30P] $\alpha$ S line, like Tg-M83[A53T] $\alpha$ S, is an inducible model of synucleinopathy that can be used to study functional characteristics of  $\alpha$ S variants.

## Conclusion

Mounting evidence suggests that the pathogenesis of PD is conceptually similar to that of prion diseases. Nevertheless, the cellular and molecular basis of the pathogenic mechanism remains poorly understood. If the prion model proves to be true, it will open up new strategies for diagnosis and novel disease-modifying therapies. Therefore, the aim of this thesis was to provide an enhanced understanding of the seeding behavior of  $\alpha$ S by using different tg mouse models of synucleinopathy.

In this thesis, we have presented results from a series of *in vivo* seeding experiments, which underlined the prion-like properties of  $\alpha$ S. Our finding that  $\alpha$ S seeds resist the fixation by formaldehyde, like prions and A $\beta$ , underpins the durable nature of  $\alpha$ S aggregates, which might contribute to the spread of disease pathology in the nervous system. However, future studies should further examine the seeding capacity of archived formalin-fixed brain tissue from PD patients to gain further insight into the relationship between the individual pathogenesis and the disease pathology.

It is unclear whether diseased CSF contains synucleinopathy-inducing seeds that potentially could serve as a disease biomarker of synucleinopathy. The present finding favors the notion that extracellular  $\alpha$ S from CSF is not seeding active and therefore might not be suitable for use as a diagnostic biomarker for the disease progression. Future experiments should be targeted towards the identification of other biomarker candidates in bodily fluids, whereby the synucleinopathy CSF may still be of great value.

Recent studies suggest that *in vitro* generated  $\alpha$ S fibrils may adopt a diversity of amyloid conformations with corresponding functional consequences, albeit these 'strains' were synthetic and the relevance to the *in vivo* situation is still unknown. From the present study, the functional characteristics of PD-linked  $\alpha$ S mutants became apparent. We can conclude from these results that tg mouse brain-derived human  $\alpha$ S variants may indeed dictate differential clinicopathological consequences. Nevertheless, experiments focusing on the structural properties of these isoforms are needed to provide final evidence for the templated conversion by non-homologous seeding *in vivo*.

---

## References

- Alpers M (2007) A history of kuru. *P N G Med J* 50:10-19.
- Aguzzi A, Heikenwalder M, Polymenidou M (2007) Insights into prion strains and neurotoxicity. *Nat Rev Mol Cell Biol* 8:552-561.
- Aguzzi A, Sigurdson C, Heikenwalder M (2008a) Molecular Mechanism of Prion Pathogenesis. *Annu Rev Pathol Mech Dis* 3:11-40.
- Aguzzi A, Baumann F, Bremer J (2008b) The Prion's Elusive Reason for Being. *Annu Rev Neurosci* 31:439-477.
- Anderson JP, Walker DE, Goldstein JM, de Laat R, Banducci K, Caccavello RJ, Barbour R, Huang J, Kling K, Lee M, Diep L, Kein PS, Shen X, Chataway T, Schlossmacher MG, Seubert P, Schenk D, Sinha S, Gai WP, Chilcote TJ (2006) Phosphorylation of Ser-129 Is the Dominant Pathological Modification of alpha-Synuclein in Familial and Sporadic Lewy Body Disease. *J Biol Chem* 281:29739-29752.
- Appel-Cresswell S, Vilarino Guell C, Encarnacion M, Sherman H, Yu I, Snah B, Weir D, Thompson C, Szu-Tu C, Trinh J, Aasly JO, Rajput A, Rajput AH, Jon Stoessel A, Farrer MJ (2013) Alpha-synuclein p.H50Q, a novel pathogenic mutation for Parkinson's disease. *Mov Disord* 28:811-813.
- Aslund A, Sigurdson CJ, Klingstedt T, Grathwohl S, Bolmont T, Dickstein DL, Glimsdal E, Prokop S, Lindgren M, Konradsson P, Holtzman DM, Hof PR, Heppner FL, Gandy S, Jucker M, Aguzzi A, Hammarström P, Nilsson KP (2009) Novel pentameric thiophene derivatives for in vitro and in vivo optical imaging of a plethora of protein aggregates in cerebral amyloidosis. *ACS Chem Biol* 4:673-684.
- Baba M, Nakajo S, Tu P-H, Tomita T, Nakaya K, Lee VM, Trojanowski JQ, Iwatsubo T (1998) Aggregation of alpha-Synuclein in Lewy Bodies of Sporadic Parkinson's Disease and Dementia with Lewy Bodies. *Am J Pathol* 152:879-884.
- Bacioglu M, Maia LF, Preische O, Schelle J, Apel A, Kaeser SA, Schweighauser M, Eninger T, Lambert M, Pilotto A, Shimshek DR, Neumann U, Kahle PJ, Staufenbiel M, Neumann M, Maetzler W, Kuhle J, Jucker M (2016) Neurofilament Light Chain in Blood and CSF as Marker of Disease Progression in Mouse Models and in Neurodegenerative Diseases. *Neuron* 91:494-496.
- Barrett PJ & Greenamyre JT (2015) Post-translational modification of alpha-synuclein in Parkinson's disease. *Brain Res* 1628:247-253.
- Bayer TA (2013) Proteinopathies, a core concept for understanding and ultimately treating degenerative disorders? *Eur Neuropsychopharmacol* 25:713-724.
- Beekes M, Thomzig A, Schulz-Schaeffer WJ, Burger R (2014) Is there a risk of prion-like disease transmission by Alzheimer- or Parkinson-associated protein particles? *Acta Neuropathol* 128:463-476.
- Bendor JT, Logan TP, Edwards RH (2013) The Function of alpha-Synuclein. *Neuron* 79:1044-1066.
- Bennett MC (2005) The role of alpha-synuclein in neurodegenerative diseases. *Pharmacol Ther* 105:311-331.

- 
- Bertoncini CW, Fernandez CO, Griesinger C, Jovin TM, Zweckstetter M (2005) Familial mutants of alpha-synuclein with increased neurotoxicity have a destabilized conformation. *J Biol Chem* 280:30649-30652.
- Bousset L, Pieri L, Ruiz-Arlandis G, Gath J, Jensen PH, Habenstein B, Madiona K, Olieric V, Böckermann A, Meier BH, Melki R (2013) Structural and functional characterization of two alpha-synuclein strains. *Nat Commun* 4:2575.
- Bousset L, Brundin P, Böckermann A, Meier B, Melki R (2016) An Efficient Procedure for Removal and Inactivation of Alpha-Synuclein Assemblies from Laboratory Materials. *J Parkinsons Dis* 6:143-151.
- Braak H, Del Tredici K, Rüb U, de Vos RA, Jansen Steur EN, Braak E (2003) Staging of brain pathology related to sporadic Parkinson's disease. *Neurobiol Aging* 24:197-211.
- Braak H, Del Tredici K (2009) Neuroanatomy and pathology of sporadic Parkinson's disease. *Adv Anat Embryol Cell Biol* 201:1-119.
- Brown P, Gibbs CJ, Jr., Gajdusek DC, Cathala F, LaBauge R (1986) Transmission of Creutzfeldt-Jakob disease from formalin-fixed, paraffin-embedded human brain tissue. *New Engl J Med* 315:1614-1615.
- Brown P, Liberski PR, Wolff A, Gajdusek DC (1990) Resistance of Scapie Infectivity to Steam Autoclaving after Formaldehyde Fixation and Limited Survival after Ashing at 360°C: Practical and Theoretical Implications. *J Infect Dis* 161:467-472.
- Brown P, Preece M, Brandel JP, Sato T, McShane L, Zerr I, Fletcher A, Will RG, Pocchiari M, Cashman NR, d'Aignaux JH, Cervenáková L, Fradkin J, Schonberger LB, Collins SJ (2000) Iatrogenic Creutzfeldt-Jakob disease at the millennium. *Neurology* 55:1075-1081.
- Brown P, Brandel J-P, Sato T, Nakamura Y, MacKenzie J, Will RG, Ladogana A, Pocchiari M, Leschek EW, Schonberger LB, (2012) Iatrogenic Creutzfeldt-Jakob disease, final assessment. *Emerging Infect Dis* 18:901-907.
- Chartier-Harlin MC, Kachergus J, Roumier C, Mouroux V, Douay X, Lincoln S, Levecque C, Larvor L, Andrieux J, Hulihan M, Waucquier N, Defebvre L, Amouyel P, Farrer M, Destée A (2004) Alpha-synuclein locus duplication as a cause of familial Parkinson's disease. *Lancet* 364:1167-1169.
- Clavaguera F, Bolmont T, Crowther RA, Abramowski D, Frank S, Probst A, Fraser G, Stalder AK, Beibel M, Staufenbiel M, Jucker M, Goedert M, Tolnay M (2009) Transmission and spreading of tauopathy in transgenic mouse brain. *Nat Cell Biol* 11:909-913.
- Cobb NJ, Surewicz WK (2009) Prion Diseases and Their Biochemical Mechanisms. *Biochemistry* 48:2574-2585.
- Cohen FE, Prusiner SB (1998) Pathologic conformations of prion proteins. *Annu Rev Biochem* 67:793-819.
- Collinge J, Clarke AR (2007) A general model of prion strains and their pathogenicity. *Science* 318:930-936.
- Collins SJ, Lawson VA, Masters CL (2004) Transmissible spongiform encephalopathies. *Lancet* 363:51-61.



- 
- Conway KA, Harper JD, Lansbury PT (1998) Accelerated in vitro fibril formation by a mutant alpha-synuclein linked to early-onset Parkinson disease. *Nat Med* 4:1318-1320.
- Conway KA, Harper JD, Lansbury PT Jr. (2000a) Fibrils formed in vitro from alpha-synuclein and two mutant forms linked to Parkinson's disease are typical amyloid. *Biochemistry* 39:2552-2563.
- Conway KA, Lee SJ, Rochet JC, Ding TT, Harper JD, Williamson RE, Lansbury PT Jr. (2000b) Accelerated oligomerization by Parkinson' diseese linked alpha-synuclein mutants. *Ann N Y Acad Sci* 920:4245.
- Corti O, Lesage S, Brice A (2011) What genetics tells us about the causes and mechanisms of Parkinson's disease. *Physiol Rev* 91:1161-1218.
- Crabtree DM, Zhang J (2012) Genetically engineered mouse models of Parkinson's disease. *Brain Res Bull* 88:13-32.
- Danzer KM, Kranich LR, Ruf WP, Cagsal-Getkin O, Winslow AR, Zhu L, Vanderburg CR, McLean PJ (2012) Exosomal cell-to-cell transmission of alpha-synuclein oligomers. *Mol Neurodegener* 7:42.
- de Laud LM, Breteler MM (2006) Epidemiology of Parkinson's disease. *Lancet Neurol* 5:525-535.
- de Rijk MC, Breteler MM, Graveland GA, Ott A, Grobbee DE, van der Meché FG, Hofman A (1995) Prevalence of Parkinson's disease in the elderly: the Rotterdam Study. *Neurology* 45:2143-2146.
- Delenclos M, Jones DR, McLean PJ, Uitti RJ (2016) Biomarkers in Parkinson's disease: Advances and strategies. *Parkinsonism Relat Disord* 22:S106-S110.
- Eisele YS, Bolmont T, Heikenwalder M, Langer F, Jacobson LH, Yan ZX, Roth K, Aguzzi A, Staufenbiel M, Walker LC, Jucker M (2009) Induction of cerebral beta-amyloidosis: intracerebral versus systemic Abeta inoculation. *Proc Natl Acad Sci U S A* 106:12926-12931.
- Eisele YS, Monteiro C, Fearn C, Encalada SE, Wiseman RL, Powers ET, Kelly JW (2015) Targeting protein aggregation for the treatment of degenerative diseases. *Nat Rev Drug Discov* 14:759-780.
- Ferreira M, Massano J (2016) An updated review of Parkinson's disease genetics and clinicopathological correlations. *Acta Neurol Scand* doi: 10.1111/ane.12616
- Fearnley JM, Lees AJ (1991) Ageing and Parkinson's disease: substantia nigra regional selectivity. *Brain* 114:2283-2301.
- Flechsigg E, Hegyi I, Enari M, Schwarz P, Collinge J, Weissman C (2001) Transmission of scrapie by steel-surface-bound prions. *Mol Med* 7:679-684.
- Forno LS (1996) Neuropathology of Parkinson's disease. *J Neuropathol Exp Neurol* 55:259-272.
- Fritsch SK, Cintron A, Ye L, Mahler J, Bühler A, Baumann F, Neumann M, Nilsson KP, Hammarström P, Walker LC, Jucker M (2014a) Abeta seeds resist inactivation by formaldehyde. *Acta Neuropathol* 128:477-484.

- 
- Fritschy SK, Langer F, Kaeser SA, Maia LF, Portelius E, Pinotsi D, Kaminski CF, Winkler DT, Maetzler W, Keyvani K, Spritzer P, Wiltfang J, Kaminski Schierle GS, Zetterberg H, Staufenbiel M, Jucker M (2014b) Highly potent soluble amyloid-beta seeds in human Alzheimer brain but not cerebrospinal fluid. *Brain* 137:2909-2915.
- Fujiwara H, Hasegawa M, Dohmae N, Kawashima A, Masliah E, Goldberg MS, Shen J, Takio K, Iwatsubo T (2002) alpha-Synuclein is phosphorylated in synucleinopathy lesions. *Nat Cell Biol* 4:160-164.
- Gajdusek DC, Gibbs CJ, Jr, Alpers M (1966) Transmission and passage of experimental "kuru" to chimpanzees. *Science* 155:212-214.
- Gao L, Tang H, Nie K, Wang L, Zhao J, Gan R, Huang J, Zhu R, Feng S, Duan Z, Zhang Y, Wang L (2015) Cerebrospinal fluid alpha-synuclein as a biomarker for Parkinson's disease diagnosis: a systematic review and meta-analysis. *Int J Neurosci* 125:645-654.
- Giasson BI, Uryu K, Trojanowski JQ, Lee VM (1999) Mutant and wild type human alpha-synucleins assemble into elongated filaments with distinct morphologies in vitro. *J Biol Chem* 274:7619-7622.
- Giasson BI, Duda JE, Quinn SM, Zhang B, Trojanowski JQ, Lee VM (2002) Neuronal alpha-synucleinopathy with severe movement disorder in mice expressing A53T human alpha-synuclein. *Neuron* 34:521-533.
- Gibb WR, Lees AJ (1988) The relevance of the Lewy body to the pathogenesis of idiopathic Parkinson's disease. *J Neurol Neurosurg Psychiatry* 51:745-752.
- Goedert M, Spillantini MG, Del Tredici K, Braak H (2013) 100 years of Lewy pathology. *Nat Rev Neurol* 9:13-24.
- Goedert M (2015) Alzheimer's and Parkinson's diseases: the prion concept in relation to assembled A $\beta$ , tau, and alpha-synuclein. *Science* 349:1255-555.
- Guo JL, Covell DJ, Daniels JP, Iba M, Stieber A, Zhang B, Riddle DM, Kwong LK, Xu Y, Trojanowski JQ, Lee VM (2013) Distinct alpha-synuclein strains differentially promote tau inclusions in neurons. *Cell* 154:103-117.
- Hamaguchi T, Noguchi-Shinohara M, Nozaki I, Nakamura Y, Sato T, Kitamoto T, Mizusawa H, Yamada M (2009) The risk of iatrogenic Creutzfeldt-Jakob disease through medical and surgical procedures. *Neuropathology* 29:625-631.
- Hawkes CH, Del Tredici K, Braak H (2007) Parkinson's disease: a dual-hit hypothesis. *Neuropathol Appl Neurobiol* 33:599-614.
- Hawkes CH, Del Tredici K, Braak H (2009) Parkinson's disease: the dual hit theory revisited. *Ann N Y Acad Sci* 1170:615-622.
- Hejjaoui M, Butterfield S, Fauvet B, Vercruysse F, Cui J, Dikiy I, Prudent M, Olschewski D, Zhang Y, Eliezer D, Lashuel HA (2012) Elucidating the role of C-terminal post-translational modifications using protein semisynthesis strategies: alpha-synuclein phosphorylation at tyrosine 125. *J Am Chem Soc* 134:5196-5210.
- Hickey P, Stacy M (2011) Available and emerging treatments for Parkinson's disease: a review. *Drug Des Devel Ther* 5:241-254.

- 
- Houlden H, Singleton AB (2012) The genetics and neuropathology of Parkinson's disease. *Acta Neuropathol* 124:325-338.
- Ibáñez P, Bonnet AM, Débarges B, Lohmann E, Tison F, Pollak P, Agid Y, Dürr A, Brice A (2004) Causal relation between alpha-synuclein gene duplication and familial Parkinson's disease. *Lancet* 364:1169-1171.
- Jones DR, Delenclos M, Baine AT, DeTure M, Murray ME, Dickson DW, McLean PJ (2015) Transmission of Soluble and Insoluble alpha-Synuclein to Mice. *J Neuropathol Exp Neurol* 74:1158-1169.
- Jucker M, Walker LC (2013) Self-propagation of pathogenic protein aggregates in neurodegenerative diseases. *Nature* 501:45-51.
- Kahle PJ, Neumann M, Ozmen L, Müller V, Jacobsen H, Schindzielorz A, Okochi M, Leimer U, van der Putten H, Probst A, Kremmer E, Kretzschmar HA, Haass C (2000a) Subcellular Localization of Wild-Type and Parkinson's Disease-Associated Mutant alpha-Synuclein in Human and Transgenic Mouse Brain. *J Neurosci* 20:6365-6373.
- Kahle PJ, Neumann M, Ozmen L, Haass C (2000b) Physiology and Pathophysiology of alpha-Synuclein. Cell Culture and Transgenic Animal Models Based on a Parkinson's Disease-associated Protein. *Ann N Y Acad Sci* 920:33-41.
- Kahle PJ (2007) alpha-Synucleinopathy models and human neuropathology: similarities and differences. *Acta Neuropathol* 115:87-95.
- Kordower JH, Chu Y, Hauser RA, Freeman TB, Olanow CW (2008) Lewy body-like pathology in long-term embryonic nigral transplants in Parkinson's disease. *Nat Med* 14:504-506.
- Krüger R, Kuhn W, Müller T, Voitalla D, Graeber M, Krösel S, Przuntek H, Epplen JT, Schöls L, Riess O (1998) Ala30Pro mutation in the gene encoding alpha-synuclein in Parkinson's disease. *Nat Genet* 18:106-108.
- Kuczius T, Groschup MH (1999) Differences in proteinase K resistance and neuronal deposition of abnormal prion proteins characterize bovine spongiform encephalopathy (BSE) and scrapie strains. *Mol Med* 5:406-418.
- Lang AE, Lozano AM (1998a) Parkinson's disease. First of two parts. *N Engl J Med* 339:1044-1053.
- Lang AE, Lozano AM (1998b) Parkinson's disease. Second of two parts. *N Engl J Med* 339:1130-1143.
- Langer F, Eisele YS, Fritschi SK, Staufienbiel M, Walker LC, Jucker M (2011) Soluble Abeta seeds are potent inducers of cerebral beta-amyloid deposition. *J Neurosci* 31:14488-14495.
- Lashuel HA, Overk CR, Oueslati A, Masliah E (2013) The many faces of alpha-synuclein: from structure and toxicity to therapeutic target. *Nat Rev Neurosci* 14:38-48.
- Lees AJ (2007) Unresolved issues relating to the shaking palsy on the celebration of James Parkinson's 250th birthday. *Mov Disord* 17:S327-S334.
- Lenart P, Krejci L (2016) DNA, the central molecule of aging. *Mutat Res* 786:1-7.

- 
- Lesage S, Brice A (2009) Parkinson's disease: from monogenic forms to genetic susceptibility factors. *Hum Mol Genet* 18:R48-R59.
- Lesage S, Anheim M, Letournel F, Bousset L, Honoré A, Rozas N, Pieri L, Madiona K, Dürr A, Melki R, Verny C, Brice A; French Parkinson's Disease Genetics Study Group (2013) G51D alpha-synuclein mutation causes a novel parkinsonian-pyramidal syndrome. *Ann Neurol* 73:459-471.
- Lewy FH (1912) Paralysis agitans. I. Pathologische Anatomie. In: Lewandowsky M (ed) *Handbuch der Neurologie* Vol. 3 Berlin, Springer 920-958.
- Li J, Uversky VN, Fink AL (2001) Effects of familial Parkinson's disease point mutations A30P and A53T on the structural properties, aggregation, and fibrillation of human alpha-synuclein. *Biochemistry* 40:11604-11613.
- Li J, Uversky VN, Fink AL (2002) Conformational behavior of human alpha-synuclein is modulated by familial Parkinson's disease point mutations A30P and A53T. *Neurotoxicology* 23:553-567.
- Li W, West N, Colla E, Pletnikova O, Troncoso JC, Marsh L, Dawson TM, Jäkälä P, Hartmann T, Price DL, Lee MK (2005) Aggregation promoting C-terminal truncation of alpha-synuclein is a normal cellular process and is enhanced by the familial Parkinson's disease-linked mutations. *Proc Natl Acad Sci U S A* 102:2162-2167.
- Li JY, Englund E, Holton JL, Soulet D, Hagell P, Lees AJ, Lashley T, Quinn NP, Rehncrona S, Björklund A, Widner H, Revesz T, Lindvall O, Brundin P (2008) Lewy bodies in grafted neurons in subjects with Parkinson's disease suggest host-to-graft disease propagation. *Nat Med* 14:501-503.
- Liu CW, Giasson BI, Lewis KA, Lee VM, Demartino GN, Thomas PJ (2005) A precipitating role for truncated alpha-synuclein and the proteasome in alpha-synuclein aggregation: implications for pathogenesis of Parkinson disease. *J Biol Chem* 280:22670-22678.
- López-Otín C, Blasco MA, Partridge L, Serrano M, Kroemer G (2013) The hallmarks of aging. *Cell* 153:1194-1217.
- Loy CT, Schofield PR, Turner AM, Kwok JB (2014) Genetics of dementia. *Lancet* 383:828-840.
- Luk KC, Kehm VM, Zhang B, O'Brien P, Trojanowski JQ, Lee VM (2012a) Intracerebral inoculation of pathological alpha-synuclein initiates a rapidly progressive neurodegenerative alpha-synucleinopathy in mice. *J Exp Med* 209:975-986.
- Luk KC, Kehm V, Carroll J, Zhang B, O'Brien P, Trojanowski JQ, Lee VM (2012b) Pathological alpha-synuclein transmission initiates Parkinson-like neurodegeneration in non-transgenic mice. *Science* 338:949-953.
- Luk KC, Covell DJ, Kehm VM, Zhang B, Song IY, Byrne MD, Pitkin RM, Decker SC, Trojanowski JQ, Lee VM (2016) Molecular and biological compatibility with host alpha-synuclein influences fibril pathogenicity. *Cell Rep* 16:3373-3387.
- Maia LF, Kaeser SA, Reichwald J, Hruscha M, Martus P, Staufenbiel M, Jucker M (2013) Changes in amyloid-beta and Tau in the cerebrospinal fluid of transgenic mice over expressing amyloid precursor protein. *Sci Transl Med* 5:194re2

- 
- Manson JC, Jamieson E, Baybutt H, Tuzi NL, Barron R, McConnell I, Somerville R, Ironside J, Will R, Sy MS, Melton DW, Hope J, Bostock C (1999) A single amino acid alteration (101L) introduced into murine PrP dramatically alters incubation time of transmissible spongiform encephalopathy. *EMBO J* 18:6855-6864.
- Masuda-Suzukake M, Nonaka T, Hosokawa M, Oikawa T, Arai T, Akiyama H, Mann DM, Hasegawa M (2013) Prion-like spreading of pathological alpha-synuclein in brain. *Brain* 136:1128-1138.
- Matsuoka Y, Vila M, Lincoln S, McCormack A, Picciano M, LaFrancois J, Yu X, Dickson D, Langston WJ, McGowan E, Farrer M, Hardy J, Duff K, Przedborski S, Di Monte DA (2001) Lack of nigral pathology in transgenic mice expressing human alpha-synuclein driven by the tyrosine hydroxylase promoter. *Neurobiol Dis* 8:535-539.
- Melki R (2015) Role of Different Alpha-Synuclein Strains in Synucleinopathies, Similarities with other Neurodegenerative Diseases. *J Parkinsons Dis* 5:2017:227.
- Meyer-Luehmann M, Coomaraswamy J, Bolmont T, Kaeser S, Schaefer C, Kilger E, Neuenchwander A, Abramowski D, Frey P, Jaton AL, Vigouret JM, Paganetti P, Walsh DM, Matthews PM, Ghiso J, Staufenbiel M, Walker LC, Jucker M (2006) Exogenous induction of cerebral beta-amyloidogenesis is governed by agent and host. *Science* 313:1781-1784.
- Morales R, Abid K, Soto C (2007) The prion strain phenomenon: Molecular basis and unprecedented features. *Biochim Biophys Acta* 1772:681-691.
- Mougenot AL, Nicot S, Bencsik A, Morignat E, Verchère J, Lakhdar L, Legastelois S, Baron T (2012) Prion-like acceleration of a synucleinopathy in a transgenic mouse model. *Neurobiol Aging* 33:2225-2228.
- Naiki H, Gejyo F (1999) Kinetic analysis of amyloid fibril formation. *Methods Enzymol* 309:305-318.
- Narhi L, Wood SJ, Steavenson S, Jiang Y, Wu GM, Anafi D, Kaufman SA, Martin F, Sitney K, Denis P, Louis JC, Wypych J, Biere AL, Citron M (1999) Both familial Parkinson's disease mutations accelerate alpha-synuclein aggregation. *J Biol Chem* 274:9843-9846.
- Neumann M, Kahle PJ, Giasson BI, Ozmen L, Borroni E, Spooren W, Müller V, Odoy S, Fujiwara H, Hasegawa M, Iwatsubo T, Trojanowski JQ, Kretschmar HA, Haass C (2002) Misfolded proteinase K-resistant hyperphosphorylated alpha-synuclein in aged transgenic mice with locomotor deterioration and in human alpha-synucleinopathies. *J Clin Invest* 110:1429-1439.
- Oeppen J, Vaupel JW (2002) Demography. Broken limits to life expectancy. *Science* 296:1029-1031.
- Paleologou KE, Oueslati A, Shakked G, Rospigliosi CC, Kim HY, Lamberto GR, Fernandez CO, Schmid A, Chegini F, Gai WP, Chiappe D, Moniatte M, Schneider BL, Aebischer P, Eliezer D, Zweckstetter M, Masliah E, Lashuel HA (2010) Phosphorylation at S87 is enhanced in synucleinopathies, inhibits alpha-synuclein oligomerization and influences synuclein-membrane interactions. *J Neurosci* 30:3184-3198.

- 
- Parchi P, Castellani R, Capellari S, Ghetti B, Young K, Chen SG, Farlow M, Dickson DW, Sima AA, Trojanowski JQ, Petersen RB, Gambetti P (1996) Molecular basis of phenotypic variability in sporadic Creutzfeldt-Jakob disease. *Ann Neurol* 39:767-778.
- Parkinson J (2002) An essay on the shaking palsy. 1817. *J Neuropsychiatry Clin Neurosci* 14:223-236; discussion 222.
- Pasanen P, Myllykanagas L, Siitonen M, Raunio A, Kaakkola S, Lyytinen J, Tienari PJ, Pöyhönen M, Paetau A (2014) Novel alpha-synuclein mutation A53E associated with atypical multiple system atrophy and Parkinson's disease-type pathology. *Neurobiol Aging* 35:2180.e1-5.
- Pattison IH (1965) Resistance of the scrapie agent to formalin. *J Comp Pathol* 75:159-164.
- Peelaerts W, Bousset L, Van der Perren A, Moskalyk A, Pulizzi R, Giugliano M, Van der Haute C, Melki R, Baekelandt V (2015) Alpha-Synuclein strains cause distinct synucleinopathies after local and systemic administration. *Nature* 522:340-344.
- Peelaerts W, Baekelandt V (2016) Alpha-Synuclein strains and the variable pathologies of synucleinopathies. *J Neurochem* 1:256-274.
- Polymeropoulos MH, Higgins JJ, Golbe LI, Johnson WG, Ide SE, Di Iorio G, Sanges G, Stenroos ES, Pho LT, Schaffer AA, Lazzarini AM, Nussbaum RL, Duvoisin RC (1996) Mapping of a gene for Parkinson's disease to chromosome 4q21-q23. *Science* 274:1197-1199.
- Polymeropoulos MH, Lavedan C, Leroy E, Ide SE, Dehejia A, Dutra A, Pike B, Root H, Rubenstein J, Boyer R, Stenroos ES, Chandrasekharappa S, Athanassiadou A, Papapetropoulos T, Johnson WG, Lazzarini AM, Duvoisin RC, Di Iorio G, Golbe LI, Nussbaum RL (1997) Mutation in the alpha-synuclein gene identified in families with Parkinson's disease. *Science* 276:2045-2047.
- Pringsheim T, Jette N, Frolkis A, Steevens TD (2014) The prevalence of Parkinson's disease: a systematic review and meta-analysis. *Mov Disord* 29:1583-1590.
- Proukakis C, Dudzik CG, Brier T, MacKay DS, Cooper JM, Millhauser GL, Houlden H, Schapira AH (2013) A novel alpha-synuclein missense mutation in Parkinson disease. *Neurology* 80:1062-1064.
- Prusiner SB (1982a) Novel proteinaceous infectious particles cause scrapie. *Science* 216:136-144.
- Prusiner SB, Cochran SP, Groth DF, Downey DE, Bowman KA, Martinez HM (1982b) Measurement of the scrapie agent using an incubation time interval assay. *Ann Neurol* 11:353-358.
- Prusiner SB (1998) Prions. *Proc Natl Acad Sci U S A* 95:13363-13383.
- Prusiner SB (2012) Cell Biology. A unifying role for prions in neurodegenerative diseases. *Science* 336:1511-1513.
- Prusiner SB (2013) Biology and Genetics of Prions Causing Neurodegeneration. *Annu Rev Genet* 47:601-623.
- Prusiner SB, Woerman AL, Mordes DA, Watts JC, Rampersaud R, Berry DB, Patel S, Oehler A, Lowe JK, Kravitz SN, Geschwind DH, Glidden DV, Halliday GM, Middleton

- 
- LT, Gentleman SM, Grinberg LT, Giles K (2015) Evidence for alpha-synuclein prions causing multiple system atrophy in humans with parkinsonism. *Proc Natl Acad Sci U S A* 112:E5308-E5317.
- Recasens A, Dehay B, Bové J, Carballo-Carbajal I, Dovero S, Pérez-Villalba A, Fernagut PO, Blesa J, Parent A, Perier C, Fariñas I, Obeso JA, Bezard E, Vila M (2014a) Lewy body extracts from Parkinson disease brains trigger alpha-synuclein pathology and neurodegeneration in mice and monkeys. *Ann Neurol* 75:351-362.
- Recasens A, Dehay B (2014b) Alpha-synuclein spreading in Parkinson's disease. *Front Neuroanat* 8:159
- Schweighauser M, Bacioglu M, Fritschi SK, Shimshek DR, Kahle PJ, Eisele YS, Jucker M (2015) Formaldehyde-fixed brain tissue from spontaneously ill alpha-synuclein transgenic mice induces fatal alpha-synucleinopathy in transgenic hosts. *Acta Neuropathol* 129:157-159.
- Singleton AB, Farrer M, Johnson J, Singleton A, Hague S, Kachergus J, Hulihan M, Peuralinna T, Dutra A, Nussbaum R, Linciln S, Crawley A, Hanson M, Maraganore D, Adler C, Cookson MR, Muentner M, Baptista M, Miller D, Blancato J, Hardy J, Gwinn-Hardy K (2003) alpha-Synuclein locus triplication causes Parkinson's disease. *Science* 302:841.
- Spillantini MG, Schmidt ML, Lee VM, Trojanowski JW, Jakes R, Goedert M (1997) Alpha-synuclein in Lewy bodies. *Nature* 388:839-840.
- Spillantini MG, Crowther RA, Jakes R, Cairns NJ, Lantos PL, Goedert M (1998) Filamentous alpha-synuclein inclusions link multiple system atrophy with Parkinson's disease and dementia with Lewy bodies. *Neurosci Lett* 31:205-208.
- Stuendl A, Kunadt M, Kruse N, Bartels C, Moebius W, Danzer KM, Mollenhauer B, Schneider A (2016) Induction of alpha-synuclein aggregate formation by CSF exosomes from patients with Parkinson's disease and dementia with Lewy bodies. *Brain* 139:481-494.
- Sutton JM, Dickinson J, Walker JT, Raven ND (2006) Methods to minimize the risks of Creutzfeldt-Jakob disease transmission by surgical procedures: where to set the standard? *Clin Infect Dis* 43:757-764.
- Taylor DM, Fraser H, McConnell I, Brown AD, Brown KL, Lamza KA, Smith GRA (1994) Decontamination studies with the agents of bovine spongiform encephalopathy and scrapie. *Arch Virol* 139:313-326.
- Taylor DM (2000) Inactivation of transmissible degenerative encephalopathy agents: A review. *Vet J* 159:10-17.
- Thomas B, Beal MF (2007) Parkinson's disease. *Hum Mol Genet* 16:R183-R194.
- Thomas JG, Chenoweth CE, Sullivan SE (2013) Iatrogenic Creutzfeldt-Jakob disease via surgical instruments. *J Clin Neurosci* 20:1207-1212.
- Thomzig A, Wagenführ K, Daus ML, Joncic M, Schulz-Schaeffer WJ, Thanheiser M, Mielke M, Beekes M (2014) Decontamination of medical devices from pathological amyloid-beta-, tau- and alpha-synuclein aggregates. *Acta Neuropathol Commun* 2:151.

- 
- Uversky VN, Li J, Fink AL (2001) Evidence for a partially folded intermediate in alpha-synuclein fibril formation. *J Biol Chem* 276:10737-10744.
- Uversky VN (2007) Neuropathology, biochemistry, and biophysics of alpha-synuclein aggregation. *J Neurochem* 103:17-37.
- Uversky VN (2008) Alpha-synuclein misfolding and neurodegenerative diseases. *Curr Protein Pept Sci* 9:507-540.
- van der Putten H, Wiederhold KH, Probst A, Barbieri S, Mistl C, Danner S, Kauffmann S, Hofele K, Spooren WP, Ruegg MA, Lin S, Caroni P, Sommer B, Tolnay M, Bilbe G (2000) Neuropathology in mice expressing human alpha-synuclein. *J Neurosci* 20:3021-6029.
- Visanji NP, Brooks PL, Hazrati LN, Lang AE (2013) The prion hypothesis in PD: Braak to the future. *Acta Neuropathol Commun* 1:2
- Walker LC, Jucker M (2015) Neurodegenerative diseases: expanding the prion concept. *Annu Rev Neurosci* 38:87-103.
- Watts JC, Giles K, Oehler A, Middleton L, Dexter DT, Gentleman SM, DeArmond SJ, Prusiner SB (2013) Transmission of multiple system atrophy prions to transgenic mice. *Proc Natl Acad Sci U S A* 110:19555-19560.
- Wiggins RC (2009) Prion stability and infectivity in the environment. *Neurochem Res* 34:158-168.
- Woerman AL, Stöhr J, Aoyagi A, Rampersaud R, Krejciova Z, Watts JC, Ohyama T, Patel S, Widjaja K, Oehler A, Sanders DW, Diamond MI, Seeley WW, Middleton LT, Gentleman SM, Mordes DA, Südhof TC, Giles K, Prusiner SB (2015) Propagation of prions causing synucleinopathies in cultured cells. *Proc Natl Acad Sci U S A* 112:E4949-4958.
- Yonetani M, Nonaka T, Masuda M, Inukai Y, Oikawa T, Hisanaga S, Hasegawa M (2009) Conversion of wild-type alpha-synuclein into mutant-type fibrils and its propagation in the presence of A30P mutant. *J Biol Chem* 284:7940-7950.
- Zarranz JJ, Alegre J, Gómez-Esteban JC, Lezcano E, Ros R, Ampuero I, Vidal L, Hoenicka J, Rodriguez O, Atarés B, Llorens V, Gomez Tortosa E, del Ser T, Muñoz DG, de Yébenes JG (2004) The new mutation, E46K, of alpha-synuclein causes Parkinson and Lewy body dementia. *Ann Neurol* 55:164-173.
- Zobeley E, Flechsig E, Cozzio A, Enari M, Weissman C (1999) Infectivity of scrapie prions bound to stainless steel surface. *Mol Med* 5:240-243.



---

## Curriculum Vitae and Bibliography

*Name* Manuel Schweighauser

*Address* Nauklerstrasse 37  
72074 Tübingen  
Germany

*Phone* +49 171 7229399

*E-Mail* manuel.schweighauser@uni-tuebingen.de

*Date of Birth* 10.04.1985

*Place of Birth* Basel, Switzerland

*Citizenship* Swiss

### Education and Academic Degrees

08/2012 – 11/2016 University of Tübingen, Hertie Institute for Clinical Brain Research / German Center for Neurodegenerative Diseases, Graduate School of Cellular & Molecular Neuroscience  
  
PhD in *Cellular & Molecular Neuroscience*  
“Exogenous induction of synucleinopathy in transgenic mice – An experimental study on the prion-like properties of  $\alpha$ -synuclein”

09/2009 – 04/2011 University of Basel, Biozentrum  
  
Master of Science in *Molecular Biology*  
“The Role of mTORC2 in Hippocampal Cell Morphology”

10/2006 – 06/2009 University of Basel, Biozentrum  
  
Bachelor of Science in *Biology*

06/2005 Gymnasium Bäumlhof, Basel  
  
High School Diploma (Matura)

---

## Publications

Bacioglu M, Maia LF, Preischle O, Schelle J, Apell A, Kaeser SA, **Schweighauser M**, Eninger T, Lambert M, Pilotto A, Shimshek DR, Neumann U, Kahle PJ, Staufenbiehl M, Neumann M, Maetzler W, Kuhle J, Jucker M. Neurofilament light chain in blood and CSF as marker of disease progression in mouse models and in neurodegenerative diseases. *Neuron*. 2016; 91(2):494-496.

**Schweighauser M\***, Bacioglu M\*, Fritschi SK, Shimshek DR, Kahle PJ, Eisele YS, Jucker M. Formaldehyde-fixed brain tissue from spontaneously ill alpha-synuclein transgenic mice induces fatal alpha-synucleinopathy in transgenic hosts. *Acta Neuropathol*. 2015; 129(1):157–159.

Thomanetz V, Angliker N, Cloëtta D, Lustenberger RM, **Schweighauser M**, Oliveri F, Suzuki N, Rüegg MA. Ablation of the mTORC2 component rictor in brain or Purkinje cells affects size and neuron morphology. *J Cell Biol*. 2013; 201(2):293–308.

## Abstracts

Bacioglu M\*, **Schweighauser M\***, Mahler J, Wegenast-Braun BM, Nilsson KPR, Schell H, Shimshek DR, Kahle PJ, Eisele YS, Jucker M (2015). Exogenous induction of alpha-synucleinopathy is governed by agent and host. **Society for Neuroscience Conference**, Chicago, USA. (Poster presentation)

**Schweighauser M\***, Bacioglu M\*, Fritschi SK, Shimshek DR, Kahle PJ, Eisele YS, Jucker M (2015). Formaldehyde-fixed brain tissue from spontaneously ill alpha-synuclein transgenic mice induces fatal alpha-synucleinopathy in transgenic hosts. **EMBO / EMBL Symposium 'Mechanism of Neurodegeneration'**, Heidelberg, Germany. (Poster presentation)

---

## Description of personal contribution

1. The work presented in the first result section of this thesis (**3.1 Seeding activity of formaldehyde-fixed  $\alpha$ -synuclein pathogens**) is based on the published manuscript:

**Schweighauser M\***, Bacioglu M\*, Fritschi SK, Shimshek DR, Kahle PJ, Eisele YS, Jucker M (2015) Formaldehyde-fixed brain tissue from spontaneously ill alpha-synuclein transgenic mice induces fatal alpha-synucleinopathy in transgenic hosts. *Acta Neuropathol* 129:157-159.

**Own contribution:** Experimental design of the study (together with M.B. and M.J.); intracerebral injections of  $\alpha$ S tg mice (together with M.B.); monitoring the health status of mice (together with M.B.); immunohistochemistry and analysis of seeded brain sections as well as fluorescence microscopy; biochemical analysis; design and figure preparation (together with M.B.); writing the manuscript (together with M.J.); \*the first two authors contributed equally to this work.

2. The work presented in the second result section of this thesis (**3.2 Seeding efficacy of CSF in comparison to soluble and insoluble  $\alpha$ -synuclein**) was performed as described below:

**Own contribution:** Experimental design of the study, CSF collection; intracerebral injections of  $\alpha$ S tg mice; monitoring the health status of mice; immunohistochemistry and analysis of seeded brain sections; biochemical analysis; design and figure preparation.

3. The work presented in the third result section of this (**3.3 Cross-seeding capacities of non-homologous mutant  $\alpha$ -synuclein seeds**) was performed as described below:

**Own contribution:** Experimental design of the study (together with Mehtap Bacioglu, Matthias Jucker, and Yvonne Eisele), intracerebral injections of  $\alpha$ S tg mice (together with Mehtap Bacioglu and Yvonne Eisele); monitoring the health status of mice; immunohistochemistry and analysis of seeded brain sections; design and figure preparation.